



## NCF4 dependent intracellular reactive oxygen species regulate plasma cell formation

Chang He<sup>a,b,c</sup>, Huqiao Luo<sup>b</sup>, Ana Coelho<sup>b</sup>, Meng Liu<sup>a,b,d</sup>, Qijing Li<sup>a,b,g</sup>, Jing Xu<sup>e</sup>, Alexander Krämer<sup>b</sup>, Stephen Malin<sup>f</sup>, Zuyi Yuan<sup>c</sup>, Rikard Holmdahl<sup>b,d,\*</sup>

<sup>a</sup> Xi'an Jiaotong University Health Science Center, Xi'an, Shaanxi, PR China

<sup>b</sup> Division of Medical Inflammation Research, Department of Medical Biochemistry and Biophysics, Karolinska Institute, Stockholm, Sweden

<sup>c</sup> Department of Cardiovascular Medicine, The First Affiliated Hospital of Xi'an Jiaotong University, Xi'an, Shaanxi, PR China

<sup>d</sup> National Joint Engineering Research Center of Biodiagnostics and Biotherapy, The Second Affiliated Hospital of Xi'an Jiaotong University, Xi'an, Shaanxi, PR China

<sup>e</sup> Department of Biochemistry and Molecular Biology, School of Basic Medical Sciences, Xi'an Jiaotong University Health Science Center, Xi'an, Shaanxi, PR China

<sup>f</sup> Department of Medicine Solna (MedS) Center for Molecular Medicine, Karolinska Institute, Stockholm, Sweden

<sup>g</sup> Department of Hematology, the First Affiliated Hospital of Xi'an Jiaotong University, Xi'an, Shaanxi, PR China

### ARTICLE INFO

#### Keywords:

Neutrophil cytosolic factor 4  
Redox regulation  
B cell  
Plasma cell  
Autoimmunity  
Oxidative eustress

### ABSTRACT

Defective reactive oxygen species (ROS) production by genetically determined variants of the NADPH oxidase 2 (NOX2) complex component, NCF4, leads to enhanced production of autoantibodies to collagen type II (COL2) and severe collagen-induced arthritis (CIA) in mice. To further understand this process, we used mice harboring a mutation in the lipid endosomal membrane binding site (R58A) of NCF4 subunit. This mutation did not affect the extracellular ROS responses but showed instead decreased intracellular responses following B cell stimulation. Immunization with COL2 led to severe arthritis with increased antibody levels in *Ncf4*<sup>58A</sup> mutated animals without significant effects on antigen presentation, autoreactive T cell activation and germinal center formation. Instead, plasma cell formation was enhanced and had altered CXCR3/CXCR4 expression. This B cell intrinsic effect was further confirmed with chimeric B cell transfer experiments and *in vitro* LPS or CD40L with anti-IgM stimulation. We conclude that NCF4 regulates the terminal differentiation of B cells to plasma cells through intracellular ROS.

### 1. Introduction

Reactive oxygen species (ROS) and its downstream metabolites are known for their roles not only as toxic agents but also as physiological regulators of biological processes. The main source of ROS is the NOX2 complex [1]. The NOX2 complex is composed of a transmembrane heterodimer, NOX2 (gp91phox, CYBB) and p22phox (CYBA), a cytosolic heterotrimer, NCF1 (p47phox), NCF2 (p67phox) and NCF4 (p40phox) as well as a small GTPase Rac (1 or 2) [2]. Upon activation, phosphorylation of NCF1 induces conformational changes, allowing the complexing of NCF2 with the transmembrane heterodimer and Rac, which enables the transfer of electrons from NADPH to molecular oxygen to produce superoxide anion, and leads to hydrogen peroxide (H<sub>2</sub>O<sub>2</sub>) production as well as other kinds of ROS [3].

To anchor the complex, both NCF1 and NCF4 interact with membrane phospholipid through their PX domains, however, they have

different preferences in phospholipid-binding specificities. NCF1 binds to phosphatidylinositol 3,4-bisphosphate and phosphatidic acid [4,5], which are mainly found in plasma membrane, while NCF4 binds to phospholipid phosphatidylinositol 3-phosphate (PtdIns3P) [4], which is mainly found in endosome and phagosome membrane [6]. Therefore, NCF1 and NCF4 direct the NOX2 complex to different cellular compartments.

Deficiency in subunits of the NOX2 complex leads to chronic granulomatous disease (CGD), a rare primary immunodeficiency disease which is characterized by severe recurrent bacterial and fungal infections as well as tissue granuloma formation [7]. Compared to classical CGD, neutrophils from patients with mutations in *NCF4* cannot kill bacteria efficiently but have an intact ability to kill fungi [8,9]. These *NCF4*-deficient patients suffer from hyperinflammation, autoimmunity and peripheral infections rather than life-threatening invasive infections. Interestingly, *in vitro*, *NCF4* deficiency impairs NADPH oxidase activity of B cells more severely, compared to mononuclear phagocytes

\* Corresponding author. Division of Medical Inflammation Research, Dept. of Medical Biochemistry and Biophysics, Karolinska Institute, Stockholm, Sweden.

E-mail address: [rikard.holmdahl@ki.se](mailto:rikard.holmdahl@ki.se) (R. Holmdahl).

<https://doi.org/10.1016/j.redox.2022.102422>

Received 17 May 2022; Received in revised form 12 July 2022; Accepted 22 July 2022

Available online 27 August 2022

2213-2317/© 2022 Published by Elsevier B.V. This is an open access article under the CC BY-NC-ND license (<http://creativecommons.org/licenses/by-nc-nd/4.0/>).

Nomenclature			
APC	antigen presenting cell	iLN	inguinal lymph node
ASC	antibody secreting cell	LLPC	long-lived plasma cell
BCR	B cell receptor	MHC II	major histocompatibility complex region class II
CGD	chronic granulomatous disease	NOX2	NADPH oxidase 2
CIA	collagen-induced arthritis	PB	plasmablast
COL2	collagen type II	PIL	pristane-induced lupus
DPI	days post immunization	PtdIns3P	phospholipid phosphatidylinositol 3-phosphate
GC	germinal center	RA	rheumatoid arthritis
GSK	GSK2795039	ROS	reactive oxygen species
H <sub>2</sub> O <sub>2</sub>	hydrogen peroxide	SLE	systemic lupus erythematosus
		SNP	single nucleotide polymorphism
		Tfh	follicular helper T

[8].

Importantly, a single nucleotide polymorphism (SNP) in *NCF1* has recently been identified [10,11], which has a major influence on a range of autoimmune diseases, including systemic lupus erythematosus (SLE) [10,12] and rheumatoid arthritis (RA) [12]. The association was not detected by genome wide association studies as the *NCF1* gene has not been sequenced due to a complicated structure with duplications. Nevertheless, a copy number variation in *NCF1* has been found associated with RA [11]. In addition, it was also found that SNPs linked to the *NCF4* gene was associated with RA [13,14]. These findings confirm previous discoveries in animal models, where *Ncf1* was found to be major gene controlling both arthritis [15,16] and lupus [17]. The NCF1 effects on murine lupus confirmed previous findings that a deletion of NCF2 leads to severe lupus in autoimmune prone mouse strains [18].

The NCF4 protein interacts with endosomal membranes rather than the plasma membrane, due to its binding specificity for PtdIns3P, and it has been shown to be involved in the activation of NOX2 complex through Fc receptors and phagocytosis [19]. The interaction with PtdIns3P is mainly mediated by the arginine on position 58 (R58) and less efficient activation of the NOX2 complex on endosomal membranes was observed with this mutation [20].

To address if the profound effects on autoimmunity were restricted to the NCF1 component, we recently showed that deletion of NCF4, as well as a mutation blocking its interaction with phospholipids, was strongly associated with collagen-induced arthritis (CIA) [21]. The deletion of NCF4 impairs the function of both NCF1 and NCF2, as these proteins are complexed. However, cells from mice with the R58A amino acid replacement mutation did not change the levels of other NOX2 complex components, showing a decreased intracellular ROS response but an increased extracellular response [21]. Interestingly, *Ncf4*<sup>R58A</sup> had a more restricted effect when tested in autoimmune conditions, with no effect in psoriatic arthritis while severely exaggerated disease was found in models of rheumatoid arthritis, such as CIA. In addition, it had a profound effect on antibody levels without disturbing the T cell response to collagen type II (COL2), suggesting there should be a direct regulation on B cell functions.

In this study, we first confirmed that the expression of cytosolic NOX2 complex subunits in B cells was not influenced by the *Ncf4*<sup>R58A</sup> mutation. This mutation preferentially influenced intracellular ROS response after PMA stimulation and had a more profound effect in B cells than in neutrophils. In the CIA model, the *Ncf4*<sup>R58A</sup> variant significantly enhanced disease severity and autoantibody production upon single immunization with COL2. During priming stage, the *Ncf4*<sup>R58A</sup> variant enhanced antibody secreting cell (ASC) formation and maturation with limited effects on antigen presentation of COL2, auto-reactive T cell activation and germinal center formation. Furthermore, COL2-specific plasma cells with *Ncf4*<sup>R58A</sup> showed altered CXCR3/CXCR4 expression and preferentially migrated to inflamed synovial tissues rather than bone marrow, which likely contributed to disease chronicity.

## 2. Results

### 2.1. Intracellular, but not extracellular ROS induction, is modified by *Ncf4*<sup>R58A</sup> in B cells

The deletion of NCF4 protein in *Ncf4*<sup>-/-</sup> mice has been reported to impair the expression of NCF1 and NCF2. Consequentially, *Ncf4*<sup>-/-</sup> cells had decreased intra and extracellular ROS production. In contrast, neutrophils with the R58A mutation in the PtdIns3P binding site of NCF4 had an unaffected expression of cytosolic NOX2 complex subunits as well as decreased intracellular ROS responses and increased extracellular ROS responses after stimulation [21]. To determine the influence of NCF4 on ROS production in B cells, we first measured the expression of cytosolic NOX2 complex subunits in B cells modified by *Ncf4*<sup>R58A</sup>. NCF1, NCF2 and NCF4 were found to be expressed in spleen B cells, at lower levels than neutrophils as expected, and were not affected by *Ncf4*<sup>R58A</sup> (Fig. 1A-C, Fig. S1A).

Next, ROS production of splenic B cells from B10Q.*Ncf4*<sup>58A/58A</sup> mice and littermate B10Q.*Ncf4*<sup>58A/R58</sup>, B10Q.*Ncf4*<sup>R58/R58</sup> mice was measured. ROS produced by neutrophils were measured simultaneously as positive controls, as they are the strongest NOX2 complex-derived ROS producers. After stimulation with PMA, both neutrophils and B cells with *Ncf4*<sup>58A/58A</sup> showed decreased intracellular ROS responses (Fig. 1D-G), whilst extracellular ROS was not affected (Fig. 1H). ROS production of neutrophils from B10Q.*Ncf4*<sup>58A/58A</sup> and B10Q.*Ncf4*<sup>58A/R58</sup> mice was 65.2% ± 3.5% and 88.8% ± 3.3% of B10Q.*Ncf4*<sup>R58/R58</sup> neutrophils respectively (Fig. 1E), while the ROS production of B10Q.*Ncf4*<sup>58A/58A</sup> and B10Q.*Ncf4*<sup>58A/R58</sup> B cells was 29.4% ± 5.2% and 77.0% ± 7.3% of B10Q.*Ncf4*<sup>R58/R58</sup> B cells (Fig. 1G), therefore showing a dose effect of *Ncf4*<sup>R58A</sup> mutation on intracellular ROS production in both B cells and neutrophils. Importantly, the normalized effect in B cells was even more pronounced than in neutrophils, suggesting that NCF4 may have a strong ROS-mediated intracellular influence on B cell function.

### 2.2. *Ncf4*<sup>58A</sup> enhances autoantibody production and disease severity in CIA

*Ncf4*<sup>58A</sup> has previously been shown to increase anti-COL2 antibody responses and disease severity in CIA [21]. To further explore the role of NCF4, we modified the CIA protocol by inducing the disease with a single priming immunization, as a booster dose of heterologous COL2 tends to enhance the immune response to the immunogen rather than allowing an autoimmune response from eroded cartilage in the joints (Fig. 2A and B). With a single priming immunization, *Ncf4*<sup>58A</sup> dramatically enhanced the disease severity as well as the susceptibility to CIA. Even a single copy of the mutation had an effect, which correlated well with intracellular ROS production level, suggesting a dose-dependent effect of the intracellular ROS response on disease severity. Interestingly, if we applied the standard protocol of CIA that includes a booster immunization by COL2 in IFA on the 35th day post immunization (DPI),

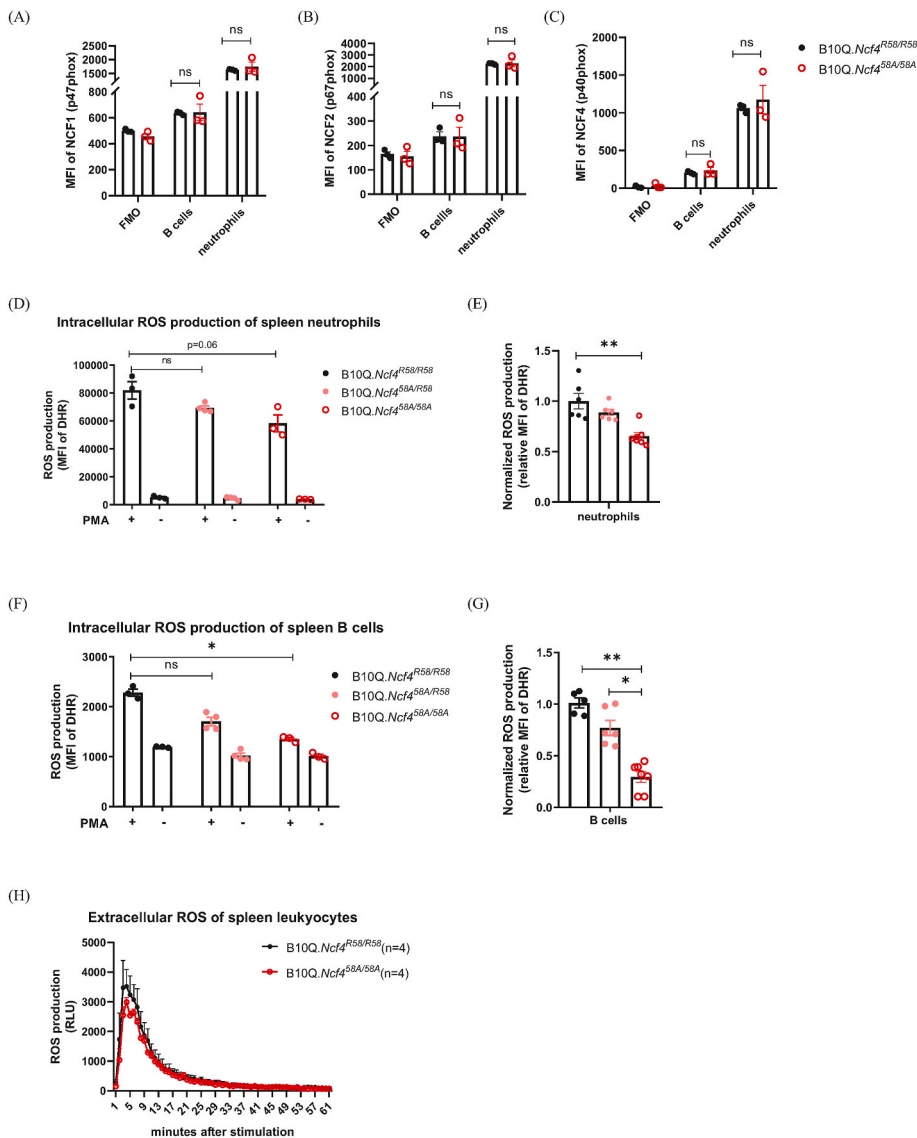


**Fig. 1. Expression of cytosolic NOX2 complex subunits and ROS production upon PMA stimulation in B10Q.Ncf4<sup>R58A/R58A</sup> mice.**

(A–C) Expression of NCF1 (A), NCF2 (B) and NCF4 (C) in spleen B cells (CD19<sup>+</sup> B220<sup>+</sup>) and neutrophils (CD11b<sup>+</sup> Ly6G<sup>+</sup>) from naive B10Q.Ncf4<sup>R58/R58</sup> and B10Q.Ncf4<sup>58A/58A</sup> mice. Samples without staining the target protein (indicated as fluorescence minus one, FMO) were used as negative controls. (D–G) Intracellular PMA-stimulated ROS production of spleen neutrophils (D) and B cells (E) from naive B10Q.Ncf4<sup>R58/R58</sup>, B10Q.Ncf4<sup>58A/R58</sup> and B10Q.Ncf4<sup>58A/58A</sup> mice. Relative ROS production of spleen neutrophils (E) and B cells (G) was calculated by  $(\text{MFI}_{\text{PMA}} - \text{MFI}_{\text{control}}) / \text{MFI}_{\text{control}}$ , then normalized to the mean of B10Q.Ncf4<sup>R58/R58</sup> group (wt). Results of relative ROS production were pooled from two independent experiments. (H) Extracellular PMA-stimulated ROS production of spleen leukocytes from naive B10Q.Ncf4<sup>R58/R58</sup> and B10Q.Ncf4<sup>58A/58A</sup> mice. FMO, fluorescence minus one; MFI, mean fluorescence intensity; DHR, dihydrorhodamine; wt, wild type.

a diminished effect of the *Ncf4*<sup>R58A</sup> mutation was seen (Fig. S2A and B).

To study the formation of autoreactive ASCs, we measured anti-COL2 antibody titers in circulating blood during priming (12 DPI), disease onset (20 DPI), established (35 DPI) and chronic (90 DPI) stages (Fig. 2C). Limited anti-COL2 antibodies were detected during priming stage and no differences were found between groups, while titers increased dramatically in *Ncf4*<sup>58A/58A</sup> mice on 20 DPI, a time point just before the disease onset. The isotypes of anti-COL2 antibodies on 20 DPI influenced by *Ncf4*<sup>58A</sup> were mainly IgG1 and IgG2b (Fig. 2D). Later in the disease development, the differences in anti-COL2 antibody titers diminished. Furthermore, the titer of anti-COL2 antibody on 20 DPI correlated with the later disease severity on 90 DPI (Fig. 2E), while the antibody titer on 90 DPI did not (Fig. 2F), suggesting that immune responses happened during priming stage is of greater importance for disease development.

To investigate whether pathogenic antibodies were produced by ASCs in situ, we measured ASCs in knee synovium on 90 DPI. CD19<sup>+</sup> B220<sup>+</sup> CD138<sup>+</sup> mature plasma cells but not CD19<sup>+</sup> B220<sup>+</sup> CD138<sup>+</sup> plasmablasts could be found in synovium of both B10Q.Ncf4<sup>58A/58A</sup> and B10Q.Ncf4<sup>R58/R58</sup> mice (Fig. 2G), with an increase of anti-COL2 ASCs from mice with *Ncf4*<sup>58A</sup> (Fig. 2H), and most of them were IgG2b and IgG1 ASCs (Fig. 2I). The bone marrow is a survival niche for long-lived plasma cells that can give rise to circulating antibodies. Therefore, we

also checked bone marrow from immunized (90 DPI) mice but we observed no effect by the *Ncf4*<sup>R58A</sup> mutation on COL2-specific ASCs (Fig. 2J and K). Finally, B10Q.Ncf4<sup>58A/58A</sup> mice had more active arthritis even at the very late stage as 90 days after immunization, which could be both a cause and result of the increased number of ASCs in the synovium.

### 2.3. T cell activation during priming stage is not affected by *Ncf4*<sup>R58A</sup>

The increased serum levels of anti-COL2 antibodies in B10Q.Ncf4<sup>58A/58A</sup> mice were IgG class-switched, suggesting that the B cell response after COL2 immunization was dependent on B-T cell interactions. To understand the mechanism of increased numbers of ASCs in *Ncf4*<sup>58A/58A</sup> mice, we first checked if antigen presentation and T cell activation during early priming stage (12 DPI) was affected. The number and major histocompatibility complex region class II (MHC II) expression on classical antigen presenting cells (APCs) (B cells, macrophages and dendritic cells) in spleen and inguinal lymph nodes (iLNs) were comparable between immunized B10Q.Ncf4<sup>R58/R58</sup> and B10Q.Ncf4<sup>58A/58A</sup> mice (Fig. 3A–D). Presentation of the MHCII molecule A<sup>i</sup> restricted major peptide of COL2 (both GalHyk264 or non-modified K264) and antigen processing of COL2 protein by naive splenocytes, was also not affected in the B10Q.Ncf4<sup>58A/58A</sup> mouse strain (Fig. 3E and F). The number of total CD4<sup>+</sup> T cells and the frequency of memory/effector/naive T cells were

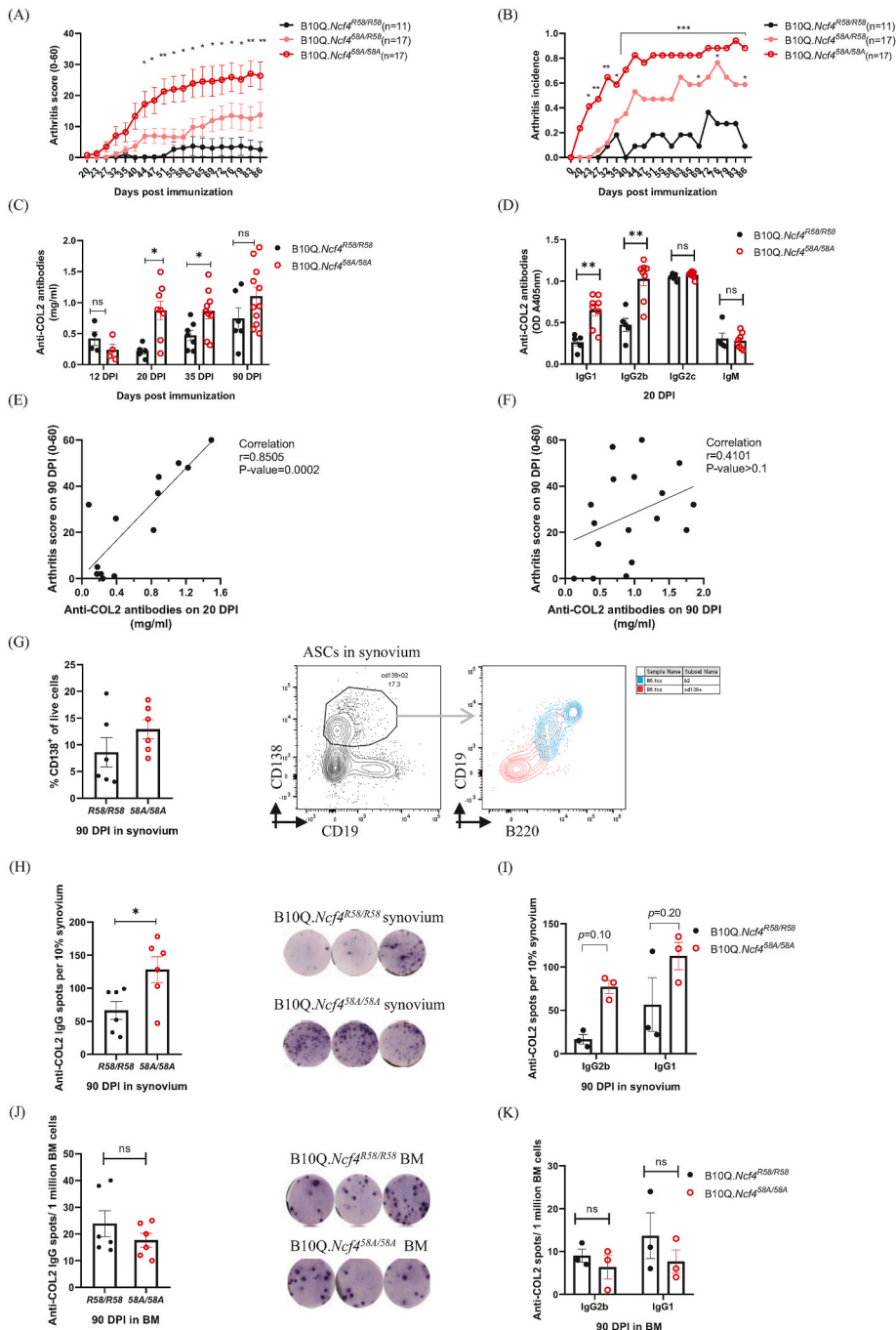


**Fig. 2.** *Ncf4*<sup>58A</sup> enhanced autoantibody production and disease severity in CIA.

(A) Disease severity and (B) incidence of rat COL2-induced arthritis (CIA) in male B10Q.*Ncf4*<sup>R58/R58</sup>, B10Q.*Ncf4*<sup>58A/R58</sup> and B10Q.*Ncf4*<sup>58A/58A</sup> mice. Results were pooled from two independent experiments. (C) Levels of total anti-COL2 antibodies in the serum from immunized B10Q.*Ncf4*<sup>R58/R58</sup> and B10Q.*Ncf4*<sup>58A/58A</sup> mice on 12, 20, 35, 90 days post immunization (DPI). Data on different DPIs were not obtained from the same batch of experiment, while all experiments were performed under the same protocol. (D) Levels of different isotypes of anti-COL2 antibodies in the serum from immunized B10Q.*Ncf4*<sup>R58/R58</sup> and B10Q.*Ncf4*<sup>58A/58A</sup> mice on 20 DPI. (E, F) The correlation between disease severity (90 DPI) and anti-COL2 antibody titers on 20 DPI (E) and 90 DPI (F) was determined using Pearson correlation analysis. (G) The frequency of ASCs (CD138<sup>+</sup>) in knee synovium from immunized B10Q.*Ncf4*<sup>R58/R58</sup> and B10Q.*Ncf4*<sup>58A/58A</sup> mice on 90 DPI and the expression of CD19, B220 on ASCs (red population). B cells (CD19<sup>+</sup>B220<sup>+</sup>, blue population) from the same sample were used as the positive control for CD19 and B220 staining. Representative FACS plots were shown. Results were pooled from two independent experiments. (H, I) Total anti-COL2 IgG ASCs (H) and anti-COL2 IgG2b, IgG1 ASCs (I) in synovium of immunized B10Q.*Ncf4*<sup>R58/R58</sup> and B10Q.*Ncf4*<sup>58A/58A</sup> mice on 90 DPI. Graph showed spots per 10% of both knee synovium. Representative ELISPOT results of total anti-COL2 IgG ASCs in knee synovium were shown. (J, K) Total anti-COL2 IgG ASCs (J) and anti-COL2 IgG2b, IgG1 ASCs (K) in bone marrow of immunized B10Q.*Ncf4*<sup>R58/R58</sup> and B10Q.*Ncf4*<sup>58A/58A</sup> mice on 90 DPI. Representative ELISPOT results of total anti-COL2 IgG ASCs in bone marrow were shown. CIA, collagen-induced arthritis; DPI, days post immunization; COL2, collagen type II; ASC, antibody secreting cell; BM, bone marrow. (For interpretation of the references to colour in this figure legend, the reader is referred to the Web version of this article.)

comparable between immunized B10Q.*Ncf4*<sup>R58/R58</sup> and B10Q.*Ncf4*<sup>58A/58A</sup> mice (Fig. 3G and H). Moreover, we observed no differences in recall responses of Th1, Th2 and Th17 cells to the rat COL2 peptide Gal-HyK264 (Fig. 3I). Taken together, *Ncf4*<sup>R58A</sup> had no detectable influence on COL2 processing and presentation, or on antigen specific T cell activation.

#### 2.4. *Ncf4*<sup>58A</sup> enhances ASC formation with minor effects on germinal center formation

Next, B cell activation and differentiation during late priming stage (day 17 after COL2 immunization) was determined in the draining inguinal lymph nodes of immunized B10Q.*Ncf4*<sup>R58/R58</sup> and B10Q.*Ncf4*<sup>58A/58A</sup> mice. The total number of B cells, or expression of the

activation marker CD86, was not affected by *Ncf4*<sup>R58A</sup> (Fig. 4A and B). However, the number of ASCs was clearly increased in B10Q.*Ncf4*<sup>58A/58A</sup> mice (Fig. 4F). Germinal center (GC) B cells showed an increased trend in terms of frequency in B10Q.*Ncf4*<sup>58A/58A</sup> mice but no significant difference in the cell number (Fig. 4C) and comparable frequencies of dark zone and light zone GC B cells were observed (Fig. 4D). Accordingly, the number of follicular helper T (Tfh) cells was not affected either (Fig. 4E). ASCs were further subtyped: CD19 and B220 were used to distinguish plasmablast (PB)(B220<sup>+</sup>), newly formed plasma cell (CD19<sup>+</sup>B220<sup>-</sup>) and resting non-dividing plasma cell [or long-lived plasma cell [22], LLPC] (CD19<sup>-</sup>B220<sup>-</sup>) (Fig. 4H). Among all the ASCs, approximately 50% were LLPCs, 30% were newly formed PCs and 10–20% were PBs (Fig. 4H). Regarding the frequency of each subpopulations in total ASCs, B10Q.*Ncf4*<sup>R58/R58</sup> mice had more

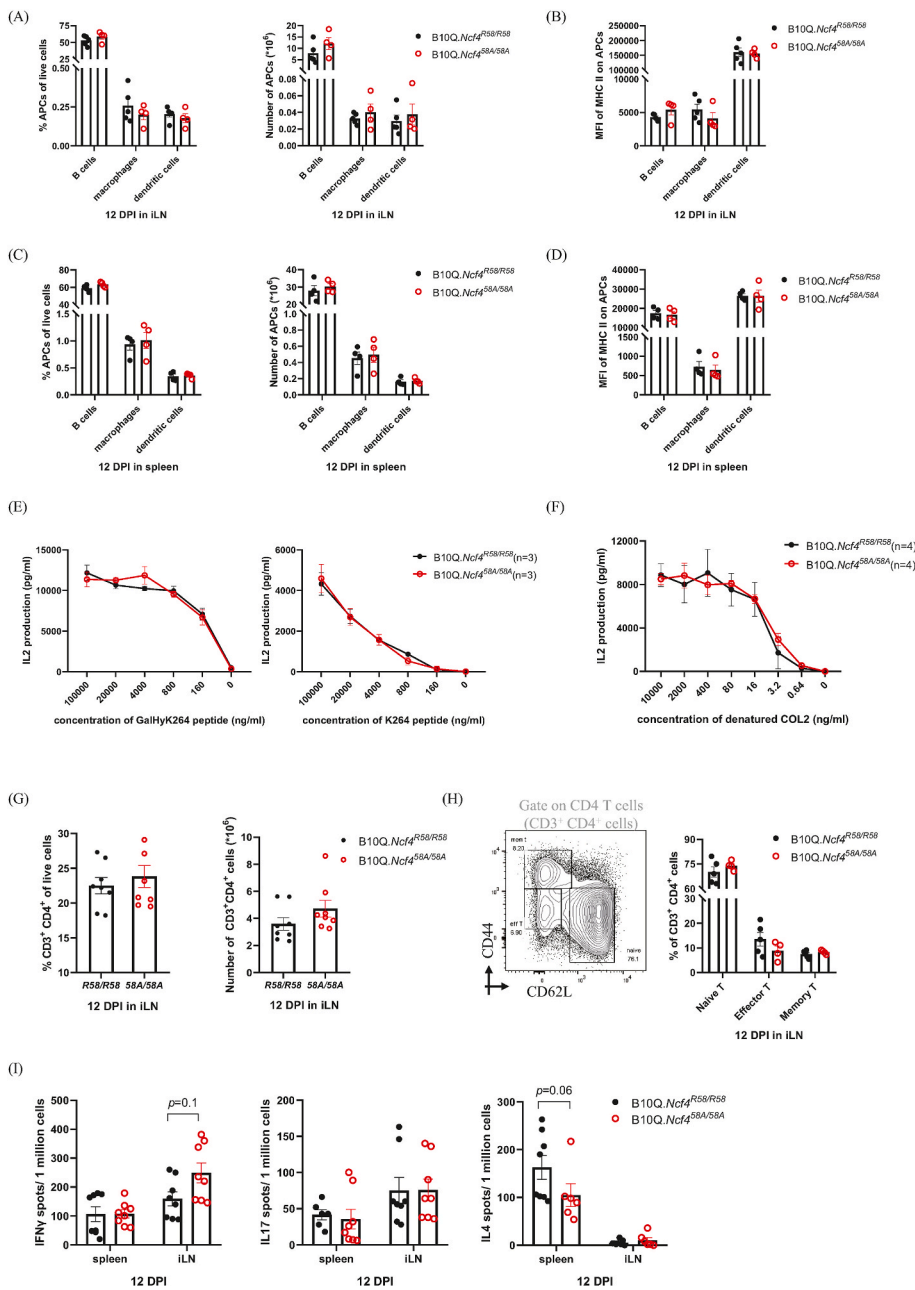


**Fig. 3.** Antigen presentation and T cell activation during priming stage were not affected by *Ncf4*<sup>R58A</sup>

(A) The frequency, number and (B) MHC II expression of B cells (CD19<sup>+</sup>B220<sup>+</sup>), macrophages (CD11b<sup>lo</sup>Ly6C<sup>-</sup>, gate on Ly6G<sup>-</sup>CD19<sup>-</sup> cells) and dendritic cells (CD11c<sup>+</sup>MHC<sup>hi</sup>, gate on Ly6G<sup>-</sup>CD19<sup>-</sup> cells) in iLN of immunized B10Q.*Ncf4*<sup>R58/R58</sup> and B10Q.*Ncf4*<sup>S8A/S8A</sup> mice on 12 DPI. (C) The frequency, number and (D) MHC II expression of B cells, macrophages and dendritic cells in spleen of immunized B10Q.*Ncf4*<sup>R58/R58</sup> and B10Q.*Ncf4*<sup>S8A/S8A</sup> mice on 12 DPI. (E, F) IL2 production by COL2-specific hybridoma incubated with spleen cells from naive B10Q.*Ncf4*<sup>R58/R58</sup> and B10Q.*Ncf4*<sup>S8A/S8A</sup> mice in the presence of GalHyK264 peptide, K264 peptide (E) or denatured COL2 (F) for 24 h. (G) The frequency and number of CD4<sup>+</sup> T cells in iLN of immunized B10Q.*Ncf4*<sup>R58/R58</sup> and B10Q.*Ncf4*<sup>S8A/S8A</sup> mice on 12 DPI. (H) Percentage of naive T cells (CD62L<sup>+</sup>CD44<sup>-</sup>), effector T cells (CD62L<sup>-</sup>CD44<sup>mid</sup>) and memory T cells (CD62L<sup>-</sup>CD44<sup>hi</sup>) in CD4<sup>+</sup> T cells in iLN of immunized B10Q.*Ncf4*<sup>R58/R58</sup> and B10Q.*Ncf4*<sup>S8A/S8A</sup> mice on 12 DPI. The representative gate was shown. (I) Spleen and iLN cells from immunized B10Q.*Ncf4*<sup>R58/R58</sup> and B10Q.*Ncf4*<sup>S8A/S8A</sup> mice (12 DPI) were stimulated with GalHyK264 peptide for 24 h and subjected to IFN $\gamma$ , IL17 and IL4 ELISPOT assay. Results were pooled from two independent experiments. APC, antigen presenting cell; iLN, inguinal lymph node.

plasmablasts and B10Q.*Ncf4*<sup>S8A/S8A</sup> mice had more LLPCs (Fig. 4H). While in terms their frequency in live cells and their cell numbers, differences were not found in PBs but only in mature PCs (Fig. 4I and J), suggesting an increase of ASCs in *Ncf4*<sup>S8A/S8A</sup> mice mainly derived from B220<sup>-</sup> mature PCs but not PBs. Antigen specific ASCs were also quantified and there were more anti-COL2 IgG ASCs in B10Q.*Ncf4*<sup>S8A/S8A</sup> mice (Fig. 4K). Interestingly, during early priming stage (12DPI), there were more anti-COL2 IgG and IgG2b ASCs in B10Q.*Ncf4*<sup>S8A/S8A</sup> mice (Fig. 4L) but no significant difference was found in general ASCs in iLN (Fig. 4G), suggesting that the role of NCF4 in preventing differentiation is stronger in autoreactive B cells than in other non-autoreactive B cells. ASCs and anti-COL2 ASCs could also be detected in bone marrow and spleen of COL2-immunized mice (17 DPI), but no differences were observed between B10Q.*Ncf4*<sup>R58/R58</sup> and B10Q.*Ncf4*<sup>S8A/S8A</sup> group (Fig. S3A-D). Similar increases were also present in the pristane-induced lupus (PIL) model. Mice received a single i.p. injection of pristane, resulting in more anti-dsDNA and anti-nucleosome IgG plasma cells in

bone marrow from immunized B10Q.*Ncf4*<sup>S8A/S8A</sup> mice compared to B10Q.*Ncf4*<sup>R58/R58</sup> mice (Fig. 4O), but with relatively unaffected number of GC B cells and Tfh cells (Fig. 4M, N) on the 10th day post injection. This suggests that the observed effect by *Ncf4*<sup>R58A</sup> on ASC formation was not restricted to COL2. Taken together, the *Ncf4*<sup>S8A</sup> mutation could enhance PC formation and autoantibody secretion, but with no or only minor effects on GC formation.

### 2.5. ASC formation regulated by *Ncf4*<sup>R58A</sup> is a B cell intrinsic effect

To investigate whether the enhanced ASC formation in COL2-immunized B10Q.*Ncf4*<sup>S8A/S8A</sup> mice is a B cell intrinsic or extrinsic effect, we performed B cell transfer experiments. B cells sorted from male B10Q.*Cd45*<sup>2</sup>.*Ncf4*<sup>S8A/S8A</sup> (all leukocytes express CD45.2) and B6NQ.*Cd45*<sup>1</sup> (all leukocytes express CD45.1, carrying wild type allele of *Ncf4*, *Ncf4*<sup>R58/R58</sup>) mice were equally mixed and transferred to B10Q.*Cd45*<sup>2</sup>. $\mu$ *Ncf4*<sup>S8A/S8A</sup> mice, which lack mature B cells. Recipient mice were

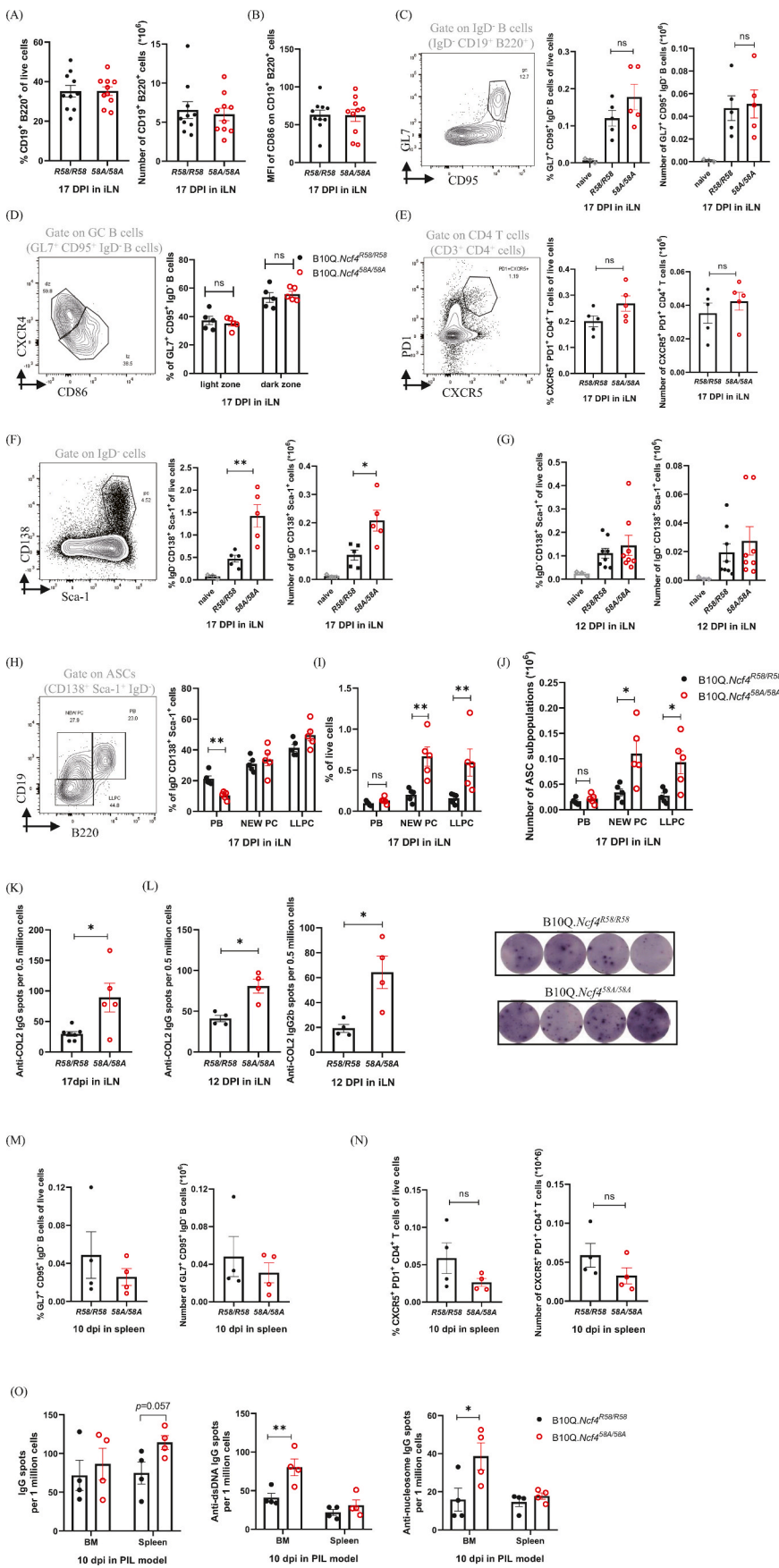


**Fig. 4.** *Ncf4*<sup>58A</sup> enhanced ASC formation with minor effects on germinal center formation

**(A)** The frequency, number and **(B)** CD86 expression of B cells in iLN from immunized B10Q.*Ncf4*<sup>R58/R58</sup> and B10Q.*Ncf4*<sup>58A/58A</sup> mice on 17 DPI. Results were pooled from two independent experiments. **(C)** The frequency and number of germinal center B cells (GL7<sup>+</sup>CD95<sup>+</sup> cells, gate on B220<sup>+</sup>CD19<sup>+</sup>IgD<sup>+</sup> population) in iLN from naive and immunized B10Q.*Ncf4*<sup>R58/R58</sup> and B10Q.*Ncf4*<sup>58A/58A</sup> mice (17 DPI). Representative gate was shown. **(D)** The frequency of dark zone (CXCR4<sup>+</sup>CD86<sup>+</sup>) and light zone (CXCR4<sup>-</sup>CD86<sup>+</sup>) GC B cells in iLN from immunized B10Q.*Ncf4*<sup>R58/R58</sup> and B10Q.*Ncf4*<sup>58A/58A</sup> mice on 17 DPI. Representative gate was shown. **(E)** The frequency and number of follicular helper T (Tfh) cells (CXCR5<sup>+</sup>PD1<sup>+</sup> cells, gate on CD3<sup>+</sup>CD4<sup>+</sup> population) in iLN from immunized B10Q.*Ncf4*<sup>R58/R58</sup> and B10Q.*Ncf4*<sup>58A/58A</sup> mice on 17 DPI. Representative gate was shown. **(F)** The frequency and number of ASCs (CD138<sup>+</sup>Sca-1<sup>+</sup>IgD<sup>+</sup>) in iLN from naive and immunized B10Q.*Ncf4*<sup>R58/R58</sup> and B10Q.*Ncf4*<sup>58A/58A</sup> mice on 17 DPI. Representative gate was shown. **(G)** The frequency and number of ASCs (CD138<sup>+</sup>Sca-1<sup>+</sup>IgD<sup>+</sup>) in iLN from naive and immunized B10Q.*Ncf4*<sup>R58/R58</sup> and B10Q.*Ncf4*<sup>58A/58A</sup> mice on 12 DPI. Results were pooled from two independent experiments. **(H, I)** The frequency of ASC subpopulations: plasmablasts (PBs) (CD19<sup>+</sup>B220<sup>+</sup>), newly formed plasma cells (NEW PCs) (CD19<sup>+</sup>B220<sup>+</sup>) and long-lived plasma cells (LLPCs) (CD19<sup>+</sup>B220<sup>-</sup>) in total ASCs **(H)** and live cells **(I)** of iLN from immunized B10Q.*Ncf4*<sup>R58/R58</sup> and B10Q.*Ncf4*<sup>58A/58A</sup> mice (17 DPI). Representative gate was shown. **(J)** The number of PBs, NEW PCs and LLPCs in iLN from immunized B10Q.*Ncf4*<sup>R58/R58</sup> and B10Q.*Ncf4*<sup>58A/58A</sup> mice (17 DPI). **(K)** Total anti-COL2 IgG ASCs in iLN from immunized B10Q.*Ncf4*<sup>R58/R58</sup> and B10Q.*Ncf4*<sup>58A/58A</sup> mice on 17 DPI. **(L)** Total anti-COL2 IgG ASCs and anti-COL2 IgG2b ASCs in iLN from immunized B10Q.*Ncf4*<sup>R58/R58</sup> and B10Q.*Ncf4*<sup>58A/58A</sup> mice on 12 DPI. Representative anti-COL2 IgG2b ELISPOT results were shown. **(M)** Mice were induced lupus using a single i.p. injection of pristane (pristane-induced lupus, PIL). The frequency and number of germinal center B cells (GL7<sup>+</sup>CD95<sup>+</sup> cells, gate on B220<sup>+</sup>CD19<sup>+</sup>IgD<sup>+</sup> population) in spleen from B10Q.*Ncf4*<sup>R58/R58</sup> and B10Q.*Ncf4*<sup>58A/58A</sup> mice were checked on 10 days post injection (dpi). **(N)** The frequency and number of Tfh cells (CXCR5<sup>+</sup>PD1<sup>+</sup> cells, gate on CD3<sup>+</sup>CD4<sup>+</sup> population) in spleen from B10Q.*Ncf4*<sup>R58/R58</sup> and B10Q.*Ncf4*<sup>58A/58A</sup> mice in PIL model (10 dpi). **(O)** Total IgG ASCs, anti-dsDNA ASCs and anti-nucleosome ASCs in bone marrow and spleen from B10Q.*Ncf4*<sup>R58/R58</sup> and B10Q.*Ncf4*<sup>58A/58A</sup> mice in PIL model (10 dpi). GC B, germinal center B cells; Tfh, follicular helper T; PB, plasmablast; NEW PC, newly formed plasma cell; LLPC, long-lived plasma cell; PIL, pristane induced lupus; dpi, days post injection.

immunized with bovine COL2, 2 days after transfer (day 0) (Fig. 5A). Purity of B cells after sorting and transfer efficacy were checked on day -2, day 0 and 16 DPI (Fig. S4A-D). Spleen, lymph nodes and bone marrow were harvested 16 days after immunization. B cells were present in the peripheral blood, spleen, lymph nodes and bone marrow (Fig. S4E-G) on 16 DPI. There were slightly more CD45.1<sup>+</sup> B cells than CD45.2<sup>+</sup> B cells in spleen, axillary lymph nodes and bone marrow, and no differences in iLN, mesenteric lymph nodes and blood (Fig. S4F). The majority of transferred B cells stayed in the spleen (Fig. S4E), possibly because they were transferred intravenously. We next measured GC and ASC formation in these mice. Most ASCs were derived from B10Q.Cd45<sup>2</sup>.Ncf4<sup>58A/58A</sup> B cells while more GCs were formed from B6NQ.Cd45<sup>1</sup> B cells (Fig. 5B and C), suggesting that NCF4 had a B cell intrinsic effect in both activation and differentiation. The ASC population was further divided into PB (9%), newly formed PC (27%) and LLPC (60%) (Fig. 5D), and the influence of Ncf4<sup>R58A</sup> on ASC formation was mainly found in newly formed PC (CD19<sup>+</sup>B220<sup>-</sup>ASC) (Fig. 5E and F).

It has been reported that, CD45.1/CD45.2 congenic bone marrow transplantation has a sex-related reconstitution bias [23,24] as CD45.1<sup>+</sup> B cells had a reduced reconstitution potential in female recipients. We also observed a related phenomenon in our experiments, despite the fact that we used mature B cells for transfer. When we checked B cells in spleen on 16 DPI, no CD45.1<sup>+</sup> B cells could be found in female recipient

mice (Fig. S4H), while in male recipient, there were comparable CD45.1<sup>+</sup> and CD45.2<sup>+</sup> B cells (Fig. S4I), suggesting it was a more pronounced sex-related effect for mature B cells transfer and reconstitution. Therefore, we only used male mice as donors and recipients. To exclude the effect of CD45.1 as well as the different backgrounds of donor mice, the experiments were repeated using both possible combinations: B cells sorted from B6NQ.Cd45<sup>1</sup> + B10Q.Cd45<sup>2</sup>.Ncf4<sup>R58/R58</sup> mice, and B cells sorted from B6NQ.Cd45<sup>1</sup> + B10Q.Cd45<sup>2</sup>.Ncf4<sup>58A/58A</sup> mice. In this experiment the recipient mice were transferred and subsequently immunized at the same time. Purity of B cells after sorting and transfer efficacy were checked on day -2 and day 0 (Fig. S4J-M, Table S1). ASC formation was checked on 16 DPI, and difference could again only be found in the group with B cells from B6NQ.Cd45<sup>1</sup> + B10Q.Cd45<sup>2</sup>.Ncf4<sup>58A/58A</sup> mice but not in the reciprocal group (Fig. 5G), confirming that the difference was dependent on Ncf4<sup>R58A</sup>.

Next, we checked if these PCs, formed after transfer, functioned normally. This time B10Q.Ncf4<sup>R58/R58</sup> B cells and B10Q.Ncf4<sup>58A/58A</sup> B cells were transferred separately into B10Q.μMT.Ncf4<sup>58A/58A</sup> mice and immunized 2 days later (Fig. 5H). There were more anti-COL2 IgG antibodies on 20 DPI and 42 DPI in mice transferred with B10Q.Ncf4<sup>58A/58A</sup> B cells, compared with mice transferred with B10Q.Ncf4<sup>R58/R58</sup> B cells (Fig. 5I).

Taken together, these data showed that B cells expressing Ncf4<sup>58A</sup>

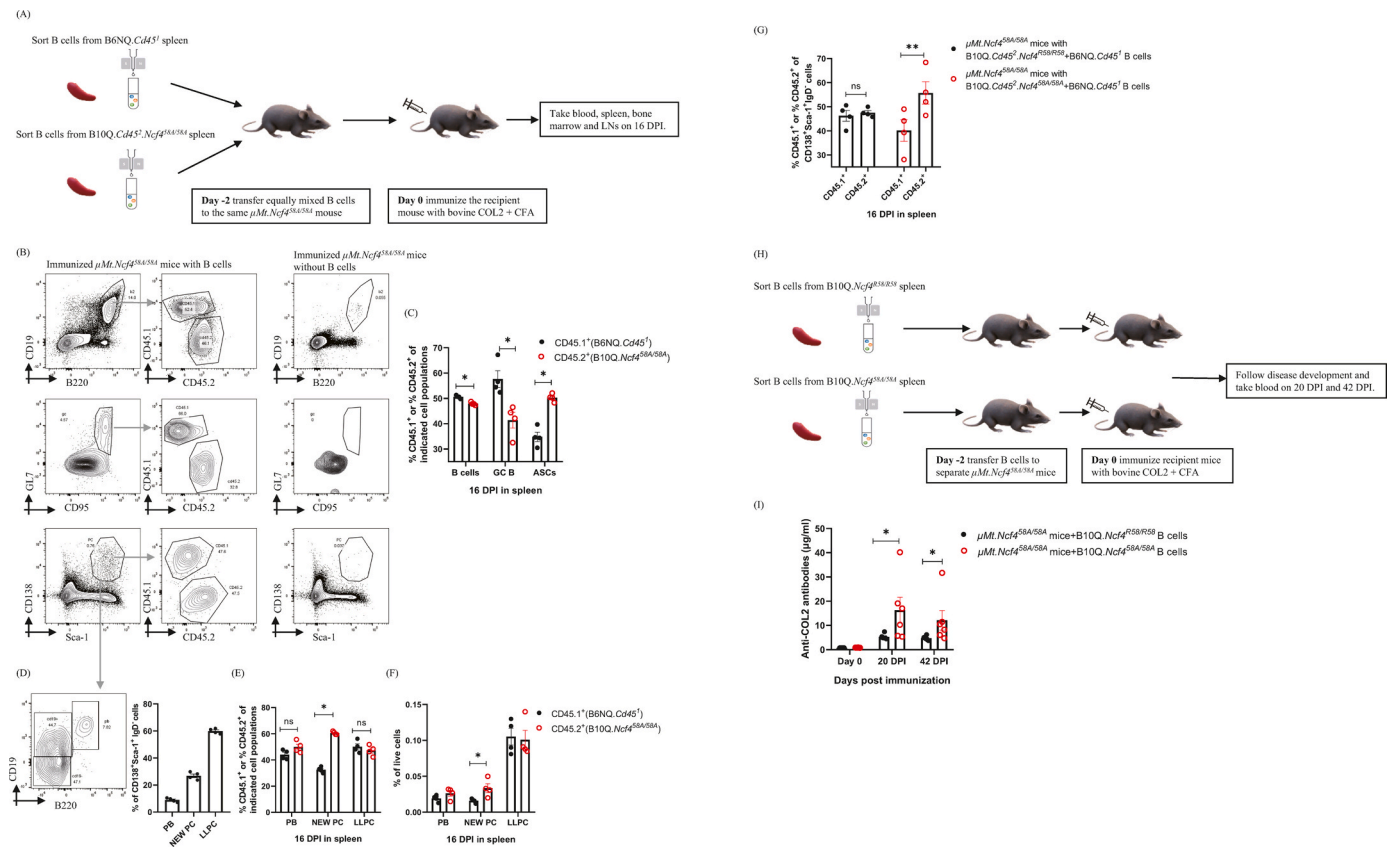


**Fig. 5.** B cells with Ncf4<sup>58A</sup> were more competitive in forming ASCs.

(A) Scheme of B6NQ.Cd45<sup>1</sup> + B10Q.Cd45<sup>2</sup>.Ncf4<sup>58A/58A</sup> chimeric B cell transfer experiment. (B) Representative plots and (C) percentage of CD45.1<sup>+</sup> and CD45.2<sup>+</sup> cells in B cells (CD19<sup>+</sup>B220<sup>+</sup>), GC B cells (CD95<sup>+</sup>GL7<sup>+</sup>, gate on IgD<sup>-</sup> B cells) and ASCs (CD138<sup>+</sup>Sca-1<sup>+</sup>, gate on IgD<sup>-</sup> cells) in the spleen of immunized recipient μMT.Ncf4<sup>58A/58A</sup> mice on 16 DPI. Immunized μMT.Ncf4<sup>58A/58A</sup> mice without transferring B cells were used as negative controls for each gating. (D) Representative plots and percentage of ASC subpopulations: PB (CD19<sup>+</sup>B220<sup>+</sup>), NEW PC (CD19<sup>+</sup>B220<sup>-</sup>) and LLPC (CD19<sup>-</sup>B220<sup>-</sup>) in ASCs in the spleen of immunized recipient μMT.Ncf4<sup>58A/58A</sup> mice on 16 DPI. (E) Frequency of CD45.1<sup>+</sup> and CD45.2<sup>+</sup> cells in PB, NEW PC and LLPC in the spleen of immunized recipient μMT.Ncf4<sup>58A/58A</sup> mice on 16 DPI. (F) Frequency of CD45.1<sup>+</sup> PB, NEW PC, LLPC and CD45.2<sup>+</sup> PB, NEW PC, LLPC in live cells in the spleen of immunized recipient μMT.Ncf4<sup>58A/58A</sup> mice on 16 DPI. (G) Percentage of CD45.1<sup>+</sup> and CD45.2<sup>+</sup> cells in ASCs (CD138<sup>+</sup>Sca-1<sup>+</sup>, gate on IgD<sup>-</sup> cells) in the spleen of immunized μMT.Ncf4<sup>58A/58A</sup> mice transferred with B10Q.Cd45<sup>2</sup>.Ncf4<sup>R58/R58</sup> + B6NQ.Cd45<sup>1</sup> or B10Q.Cd45<sup>2</sup>.Ncf4<sup>58A/58A</sup> + B6NQ.Cd45<sup>1</sup> B cells on 16 DPI. (H) Scheme of B10Q.Ncf4<sup>R58/R58</sup> and B10Q.Ncf4<sup>58A/58A</sup> B cell transfer experiment. (I) Levels of anti-COL2 antibodies in the serum from immunized recipient μMT.Ncf4<sup>58A/58A</sup> mice transferred with B10Q.Ncf4<sup>R58/R58</sup> B cells or B10Q.Ncf4<sup>58A/58A</sup> B cells on day 0, 20 DPI and 42 DPI.

preferentially differentiated to functional plasma cells secreting auto-reactive anti-COL2 antibodies.

2.6. Differentiation of *Ncf4*<sup>58A</sup>-expressing B cells to plasmablasts is promoted by their lower intracellular ROS level

We established an *in vitro* system to identify the conditions whereby *Ncf4*<sup>58A</sup> could enhance the PC differentiation. We cultured B cells for 3 days with various known stimuli (LPS, CD40L i.e., CD40L expressing fibroblasts, IL21+CD40L, anti- $\mu$ +IL21+CD40L, IL4+IL21+CD40L or IL4+IL21+anti- $\mu$ +CD40L) with no effect on cell viability between *Ncf4*<sup>58A/58A</sup> and *Ncf4*<sup>R58/R58</sup> groups (Fig. S5A). After 3 days LPS stimulation, B cells from B10Q.*Ncf4*<sup>58A/58A</sup> spleen clearly formed more plasmablasts both in terms of frequency and cell number (Fig. 6A). There were also more IgM in the supernatant of cultures with B10Q.*Ncf4*<sup>58A/58A</sup> B cells (Fig. 6B). In the CD40L stimulating group, the results were however not consistent. When stimulating with CD40L, IL21, with or

without (w/wo) IL4, no difference was found between B10Q.*Ncf4*<sup>R58/R58</sup> and B10Q.*Ncf4*<sup>58A/58A</sup> B cells. However, if we added anti- $\mu$  stimulation in this system, we found more plasmablasts formed from B cells with *Ncf4*<sup>58A/58A</sup> (Fig. 6C). Because anti- $\mu$  antibody neutralized Ig secretion, we could not observe antibody differences in the supernatant (Fig. 6D). These results suggest that *Ncf4*<sup>58A</sup> promotes ASC formation if stimulated through the TLR4 or the B cell receptor (BCR) pathway.

Next, we determined if stimulating TLR4 or BCR could activate the NOX2 complex and if it was NCF4-dependent. Intracellular ROS production of stimulated B cells was measured by dihydrorhodamine (DHR) assay. We found that LPS activation of B cells with *Ncf4*<sup>58A/58A</sup> led to a lower ROS response than *Ncf4*<sup>R58/R58</sup> B cells (Fig. 6F). Although CD40 ligation was reported to be able to induce ROS burst through the NOX2 complex [25], ROS production stimulated by CD40L+IL21 w/wo IL4 was not affected by *Ncf4*<sup>R58A</sup>. However, stimulation through the B cell receptor induced intracellular ROS production at a lower level in *Ncf4*<sup>58A/58A</sup> B cells (Fig. 6E), similar to the LPS stimulation (Fig. 6F).

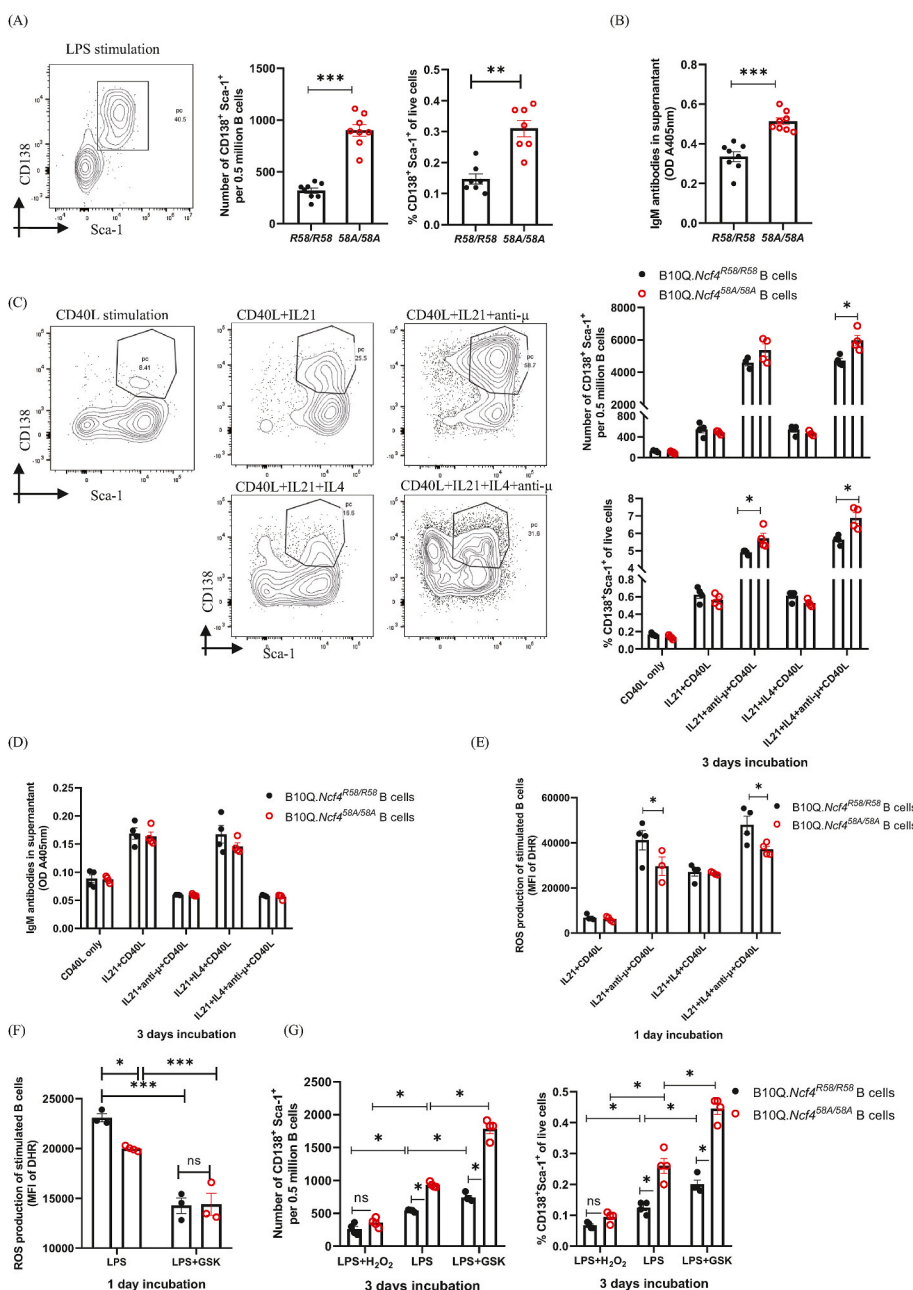


Fig. 6. Differentiation of *Ncf4*<sup>58A</sup>-expressing B cells to plasmablasts *in vitro* was promoted by their lower intracellular ROS level

(A) The number and frequency of plasmablasts within B10Q.*Ncf4*<sup>R58/R58</sup> and B10Q.*Ncf4*<sup>58A/58A</sup> B cells after stimulated with LPS for 84 h. The representative gate was shown. (B) Secreted IgM in the culture supernatant of B10Q.*Ncf4*<sup>R58/R58</sup> and B10Q.*Ncf4*<sup>58A/58A</sup> B cells after stimulated with LPS for 84 h. (C) The number and frequency of plasmablasts within B10Q.*Ncf4*<sup>R58/R58</sup> and B10Q.*Ncf4*<sup>58A/58A</sup> B cells after stimulated with irradiated CD40L expressing fibroblasts (CD40L), CD40L+IL21; CD40L+IL21+anti- $\mu$ ; CD40L+IL21+IL4 or CD40L+IL21+IL4+anti- $\mu$  for 84 h. Representative gates were shown. (D) Secreted IgM in the culture supernatant of B10Q.*Ncf4*<sup>R58/R58</sup> and B10Q.*Ncf4*<sup>58A/58A</sup> B cells after stimulated with CD40L, CD40L+IL21; CD40L+IL21+anti- $\mu$ ; CD40L+IL21+IL4 or CD40L+IL21+IL4+anti- $\mu$  for 84 h. (E) Intracellular ROS production of B10Q.*Ncf4*<sup>R58/R58</sup> and B10Q.*Ncf4*<sup>58A/58A</sup> B cells stimulated by CD40L+IL21; CD40L+IL21+anti- $\mu$ ; CD40L+IL21+IL4 or CD40L+IL21+IL4+anti- $\mu$  for 1 day. (F) Intracellular ROS production of B10Q.*Ncf4*<sup>R58/R58</sup> and B10Q.*Ncf4*<sup>58A/58A</sup> B cells stimulated by LPS and LPS + GSK2795039 (GSK) for 1 day. (G) The number and frequency of plasmablasts within B10Q.*Ncf4*<sup>R58/R58</sup> and B10Q.*Ncf4*<sup>58A/58A</sup> B cells stimulated with LPS in the presence of GSK or H<sub>2</sub>O<sub>2</sub> (during 40 h–84 h of incubation). GSK, GSK2795039.

To confirm that this effect on differentiation was ROS dependent, we added the NOX2 complex inhibitor GSK2795039 (GSK) or  $H_2O_2$  to LPS-stimulated B cells at the later differentiation stage (40 h–84 h of incubation) [26]. As shown in Fig. 6F, GSK could inhibit ROS production from NOX2 complex effectively. After 3 days incubation, there were more plasmablasts formed in both  $Ncf4^{R58/R58}$  and  $Ncf4^{58A/58A}$  groups inhibited with GSK (Fig. 6G). As  $Ncf4^{58A}$  only partly decreased ROS production, a further decrease of intracellular ROS by GSK enhanced plasmablasts formation further. After adding  $H_2O_2$ , the number of plasmablasts decreased in both groups and no differences were observed between  $Ncf4^{R58/R58}$  and  $Ncf4^{58A/58A}$  groups anymore (Fig. 6G). These results confirmed that the regulation by  $Ncf4^{R58A}$  on ASC formation operated through intracellular ROS production.

## 2.7. Altered expression of CXCR3 and CXCR4 on ASCs from B cells with $Ncf4^{58A}$

The increased number of ASCs formed in draining lymph node follicles of  $Ncf4^{58A/58A}$  mice migrated preferentially to the inflamed joint synovial tissues and we next attempted to explain this migration pattern.

We observed a decrease in the number of ASCs (Fig. S6A) and almost no PBs (Fig. S6C) in iLN on 20 DPI compared to that on 17 DPI (Fig. S6B), suggesting that the priming B cell responses were mostly completed and ASCs had migrated out of iLNs before 20 DPI. Next, we determined CXCR3 and CXCR4 expression on ASCs formed from B10Q. $Ncf4^{R58/R58}$  and B10Q. $Ncf4^{58A/58A}$  B cells, as CXCR4 homes ASCs to bone marrow, while CXCR3 drives ASCs to inflamed tissues [27]. In the chimeric B cell transfer experiments (performed in Fig. 5A), CXCR4 was upregulated during B cell differentiation and ASC maturation (Fig. 7A). B cells with  $Ncf4^{58A/58A}$  expressed higher level of CXCR4 while this effect was gradually diminished as B cell differentiated to PBs and PCs. Notably, the long-lived PCs (CD19<sup>+</sup>B220<sup>-</sup>) with  $Ncf4^{58A/58A}$  showed lower expression of CXCR4 compared to LLPCs from B10Q. $Ncf4^{R58/R58}$  B cells (Fig. 7A). CXCR3 expression on ASCs from B10Q. $Ncf4^{R58/R58}$  B cells was downregulated as PBs matured to LLPCs, but this regulation was impaired by  $Ncf4^{58A}$ , and the CXCR3 expression remained relatively

higher on mature plasma cells from B10Q. $Ncf4^{58A/58A}$  B cells (Fig. 7B). To investigate how CXCRs were induced, we stimulated freshly isolated B cells *in vitro* with different stimuli. After LPS stimulation, PBs derived from B10Q. $Ncf4^{58A/58A}$  B cells showed lower CXCR4 expression and comparable CXCR3 expression compared to plasmablasts derived from B10Q. $Ncf4^{R58/R58}$  B cells (Fig. 7C). With CD40L stimulation, differences could only be found when stimulated together with anti- $\mu$ . Anti- $\mu$  stimulation downregulated CXCR3 and CXCR4 expression on CD40L+IL21+IL4 induced plasmablasts, while plasmablasts derived from B10Q. $Ncf4^{58A/58A}$  B cells remained a relatively higher level of CXCR3 expression compared to plasmablasts derived from B10Q. $Ncf4^{R58/R58}$  B cells (Fig. 7D), suggesting the downregulation of CXCR3 might be operated through the antigen receptor pathway and this regulation could be influenced by  $Ncf4^{R58A}$ . Taken together, these results showed that  $Ncf4^{58A}$  not only enhanced ASC formation but also influenced its migration patterns.

## 3. Discussion

To clarify the importance of genetic polymorphisms associated with NOX2 complex in B cell dependent autoimmune diseases requires a greater understanding of how NOX2 complex-derived ROS regulate B cells. By studying the effect of a mutation (R58A) on  $Ncf4$  which results in a replacement of an amino acid interacting with endosomal lipid membranes, we could investigate the role of intracellular ROS on B cell activation. We found that the decreased intracellular ROS due to the  $Ncf4^{58A}$  mutation did not affect interactions with T cells but could promote ASC formation and maturation to plasma cells. These cells produced autoreactive COL2-specific antibodies and preferentially migrated to inflamed synovial tissues rather than bone marrow, where they likely contributed to sustained disease and chronicity.

NCF4 (alternatively named p40phox) is a cytosolic protein which together with NCF1 and NCF2 adheres to the membrane NOX2 complex component to induce a ROS response. A role of NCF4 is to preferentially direct the cytosolic NCF1-NCF2-NCF4 proteins to endosomal membranes to activate the NOX2 complex intracellularly. An arginine

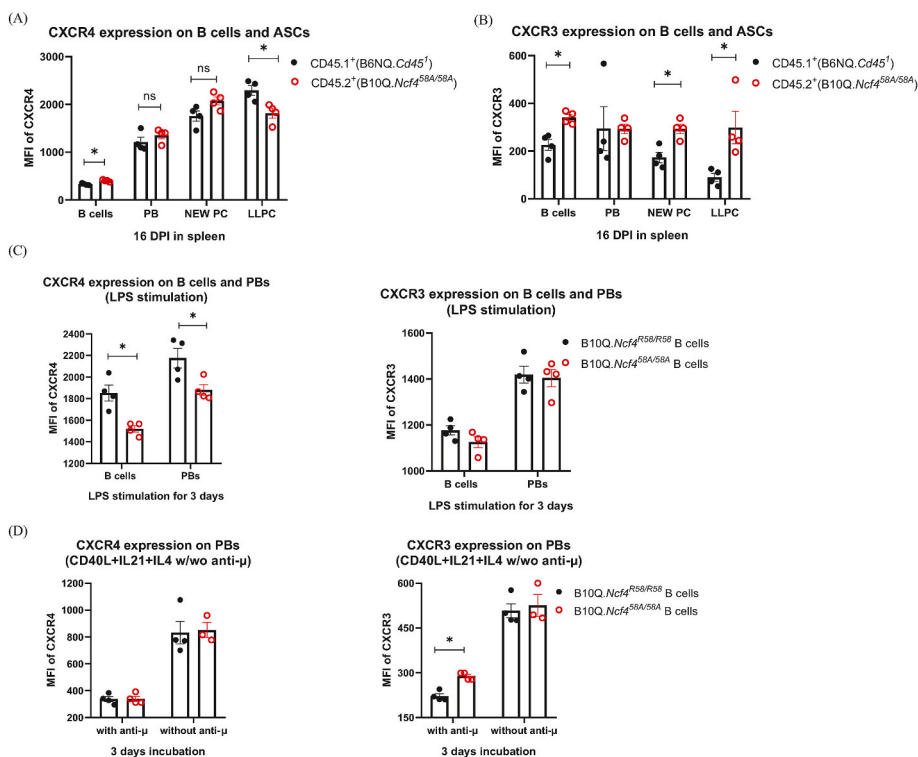


**Fig. 7. Altered expression of CXCR3 and CXCR4 on ASCs differentiated from B cells with  $Ncf4^{R58A}$**  (A, B) Expression of CXCR4 (A) and CXCR3 (B) on B cells, PBs (CD19<sup>+</sup>B220<sup>+</sup> ASCs [IgD<sup>+</sup>CD138<sup>+</sup>Sca-1<sup>+</sup>]), NEW PCs (CD19<sup>+</sup>B220<sup>-</sup> ASCs) and LLPCs (CD19<sup>+</sup>B220<sup>-</sup> ASCs) from B6NQ.Cd45<sup>+</sup> + B10Q.Cd45<sup>-2</sup>. $Ncf4^{58A/58A}$  chimeric B cell transfer experiment (experiments performed in Fig. 5A). (C) Expression of CXCR4 and CXCR3 on B cells and PBs from LPS-induced B cell differentiation experiments (experiments performed in Fig. 6A). (D) Expression of CXCR4 and CXCR3 on PBs induced by CD40L+IL21+IL4 with or without anti- $\mu$  for 3 days (experiments performed in Fig. 6C). w/wo, with or without.

replacement to an alanine at position 58 affects NCF4 adhesion to phospholipid phosphatidylinositol 3-phosphate (PtIns3P) [28] resulting in reduction of intracellular ROS responses, whereas knockout of NCF4 protein reduces NCF1 and NCF2 components expression leading to blockage of both intra and extracellular ROS responses. The *m1j* mutation in *Ncf1*, which results in a non-functional truncated protein and blocking of the lipid membrane adhesion, also reduces both intra and extracellular ROS responses, and has a profound effect on tolerance and autoimmune diseases [29]. Thus, the *Ncf4*<sup>R58A</sup> mutation provides a unique opportunity to understand the effects of intracellular ROS responses by the NOX2 complex.

Previously, we have shown that ROS produced by antigen presenting cells could oxidize thiols on and inside T cells [30], thereby protect against autoimmune arthritis models. Such a mechanism is dependent on NCF1 while the observation here suggests that NCF4, affecting intracellular ROS only, cannot mediate such protective effects on T cells in CIA. However, human NCF4-deficient (*NCF4*<sup>R105Q</sup>) B cells displayed a reduced capacity of presenting several exogenous antigens while presentation of membrane autoantigens was efficient [31]. Taken together, the influence of NCF4 on antigen presentation differs by antigen specificity and NCF4 may skew the epitope selection.

Where exactly the activation of the NOX2 complex happens during B cell differentiation is however not clear. As the activation requires interaction with antigens, there are several phases where this could occur: extrafollicular interaction with antigens, the interaction with T cells at T-B border, and the repetitive activation during the germinal center reaction. All these interactions can lead to the differentiation towards plasmablasts. Plasmablasts from an extrafollicular responses typically peak 4–6 days after immunization while plasmablasts produced from the GC response peaks 2 weeks after immunization [32]. In our study, we observed an increase in PC formation at the priming stages accompanied with sustained higher isotype-switched anti-COL2 antibody titers in mice with *Ncf4*<sup>58A</sup>. As the half-life of most plasmablasts is only a few days [33], the observation that cells secreting anti-COL2 IgG in the synovial tissues 90 days after primary immunization most likely reflects that they ended up as long-lived plasma cells secreting pathogenic antibodies in the targeted cartilaginous joints. Studies have suggested that long-lived plasma cells are mostly derived from an authentic germinal center reaction [32]. Thus, most likely, the *Ncf4*<sup>58A</sup> mutation also promotes plasma cell formation from the germinal center reaction.

The migration of plasma cells to the joints is compatible with the prolonged chronic arthritis seen in the *Ncf4*<sup>58A</sup> mutated mice. It is well recognized that chronic inflammation could lead to modulation of chemokine receptor expression on B cells and plasma cells [34,35]. CXCR3 expression of B cells and plasma cells is up-regulated in rheumatoid arthritis and systemic lupus erythematosus [36]. However, our study showed that CXCR3 expression on B cells and ASCs could be regulated intrinsically before the inflammation occurred. NCF4-dependent ROS induced by BCR ligation is needed for controlling the expression of CXCR3, indicating another aspect of redox regulation on B cell differentiation.

The COL2-B cells are autoreactive. They secrete pathogenic antibodies binding cartilage *in vivo*. Nevertheless, COL2-B cells are positively selected in the bone marrow, which was confirmed here by the presence of these cells in healthy mice [37]. It means that COL2 autoreactive B cells are already selected and present at the time of the COL2 immunization. Indirect evidence argues for that such B cells are regulatory [37], but if they differentiate to plasma cells, they can secrete pathogenic antibodies. It is possible that ROS induced during cell activation in the follicle, hinder the cells to differentiate to plasma cells and therefore protecting from disease enhancement. This could be generalized to all autoreactive B cells with a potential to produce autoantibodies, both natural polyreactive antibodies, as in lupus, and more specific cartilage specific antibodies, as in arthritis. To drive B cells to plasma cells we immunized the mice with rat or bovine COL2, which activates COL2-reactive T cells, thereafter activating COL2-reactive B cells.

Decreased intracellular ROS in *Ncf4*<sup>58A</sup> COL2-reactive B cells lowered the threshold for differentiating to plasma cells which could secrete pathogenic antibodies, leading to arthritis.

The oxygen metabolites that mediates signaling from the ROS induction is hydrogen peroxide, due to its sustained stability, which can oxidize selected sets of thiols on proteins and signaling pathways of the B cells [38]. There are however 20–40,000 such thiols in a B cell and it is likely that numerous interacting pathways can be affected [39], reaching a high level of complexity. BCR signaling plays a central role in controlling B cell fate decisions. Depending on the context, BCR ligation could lead to cell survival, apoptosis, proliferation or differentiation [40]. ROS has been shown to augment BCR signaling by inhibiting the activity of protein tyrosine phosphatase which negatively regulates BCR signaling [41]. NOX2 complex is responsible for generating the rapid initial production of ROS [42] while BCR proximal signaling and downstream signaling pathways are not affected by NOX2 [43,44]. Bertolotti et al. showed that *gp91<sup>phox</sup>*<sup>-/-</sup> B cells had impaired IgM secretion upon LPS stimulation [38] possibly because an early oxidative step was necessary to start the differentiation program [26]. In late-differentiating B cells, antioxidant induced an increase in antibody production [42], suggesting NOX2-derived ROS play a dule role in different stages of B cell differentiation. However, exactly how NOX2-derived hydrogen peroxide targets different pathways can only be solved on a higher level of complexity involving interactions of thousands of redox regulated targets in different interacting pathways.

#### 4. Conclusions

This study shows that B cells are regulated by intrinsically produced ROS, derived from the NOX2 complex and modified by NCF4. Mutations affecting an arginine at position 58 on NCF4 regulates intrinsic oxidative burst in B cells, driving plasma cells formation and influencing their migration patterns, which is a risk factor for the development of autoimmune manifestations.

#### 5. Materials and methods

##### 5.1. Mice

Founders of *Ncf4*<sup>R58A/R58A</sup> mice [28] were generously provided by Phillip T. Hawkins (Babraham Institute, Cambridge, UK) and crossed with C57BL/10.Q/*rhd* mice (abbreviated B10Q.*Ncf4*<sup>R58A/R58A</sup>) for more than 10 generations to obtain an arthritis-permissive major histocompatibility complex type II (MHC II) A<sup>q</sup> haplotype. B10Q.*Ncf4*<sup>58A/58A</sup> mice were obtained from heterozygous breeding and cohoused with heterozygous and wild-type littermate controls (indicated as B10Q.*Ncf4*<sup>58A/R58</sup> and B10Q.*Ncf4*<sup>R58/R58</sup>). *Cd45*<sup>1</sup> mice (B6.SJL-*Ptprc*<sup>a</sup> *Peprc*<sup>b</sup>/BoyJ) and *μMt*<sup>-/-</sup> mice (B6.129S2-*Ighm*<sup>tm1Cgn</sup>/J) were purchased from Jackson Laboratory. They were crossed with C57BL/6N.Q mice (abbreviated B6N.Q.*Cd45*<sup>1</sup>) and B10Q mice (abbreviated B10Q.*μMt*<sup>-/-</sup>) respectively for more than 10 generations to obtain the H2-A<sup>q</sup> haplotype. Then, B10Q.*μMt*<sup>-/-</sup> mice were crossed with B10Q.*Ncf4*<sup>58A/58A</sup> mice to obtain B cell deficient mice with *Ncf4*<sup>58A/58A</sup> background (abbreviated *μMt*<sup>-/-</sup>.*Ncf4*<sup>58A/58A</sup>).

Genotype of B10Q.*Ncf4*<sup>R58A/R58A</sup> mice was determined by qPCR with a primer set of forward 5' CAAAAGGAGGGTCCAAGTATCTCA 3', reverse 5' CAAACCGCTCCTCGAGCTT 3' and two specific dye-tagged Taqman probe TACCGGCCTATC [FAM] and TACCGCCGCTATC [VIC]. Genotype of B10Q.*μMt*<sup>-/-</sup> mice was determined by PCR with a primer set of 5' CCG TCT AGC TTG AGC TAT TAG G 3', 5'GAA GAG GAC GAT GAA GGT GG3', and 5' TTG TGC CCA GTC ATA GCC GAA T 3', which was re-confirmed that no B cells could be found in peripheral blood by staining anti-CD19, anti-B220 and checking by flow cytometry. Genotype of *Cd45*<sup>1</sup> mice was determined by CD45.1/CD45.2 expression on leukocytes in peripheral blood. White blood cells were stained with anti-CD45.1 and anti-CD45.2 and checked by flow cytometry.

All mice were kept under controlled temperature and humidity with a 12-h light-dark regimen environment in polystyrene cages (IVF) under specific pathogen free condition in the animal section of medical inflammation research at the Karolinska Institute, Stockholm. Experiments followed the ARRIVE guidelines [45].

### 5.2. Antibodies and flow cytometry

Antibodies were purchased from BD Bioscience, Biolegend, and EBioscience, including anti-CD19(1D3), anti-CD45R(B220)(RA3-6B2), anti-IgM(I1-41), anti-IgD(11-26c.2a), anti-CD117(c-kit)(2B8), anti-CD2(RM2-5), anti-CD45(30-F11), anti-CD93(AA4.1), anti-CD23(2G8), anti-CD21/CD35(7E9), anti-CD3e(145-2C11), anti-CD4(RM4-5), anti-CD62L(MEL-14), anti-CD44(IM7), anti-CD8(53-6.7), anti-CD11b(M1/70), anti-CD11c(N418), anti-Ly6C(AL-21), anti-Ly6G(1A8), anti-H-2, I-A/I-E(2G9), anti-F4/80(RM8), anti-CD138(281-2), anti-Ly6A/E(Sca-1)(D7), anti-Ly77(GL7), anti-CD95(15A7), anti-CD45.1(A20), anti-CD45.2(104), anti-CD184(CXCR4)(L276F12), anti-CD86(GL1), anti-CD183(CXCR3)(CXCR3-173), anti-CXCR5(CD185)(SPRCL5), anti-CD279(PD-1)(RMP1-30) with the fluorescence FITC, PE, PerCP-Cy5.5, PE-Cy7, APC, Alexa Fluor 700, APC-Cy7, Pacific Blue, BV605 or BV650. Dead cells were excluded by fixable near-IR dead cell stain kit (Molecular Probes, #L34976B). Briefly, for staining markers on cell surface, single cell suspension was obtained from spleen, lymph nodes and bone marrow. Spleen and bone marrow cells were first incubated with ammonium chloride-potassium (ACK) buffer (homemade) for 5min at RT to lyse red blood cells. Then, cells were washed, incubated with Fcy receptor blocker (24G2) for 10min at RT followed by 20min surface markers staining in dark on ice. For intracellular staining of NOX2 complex cytosolic subunits, cells were first stained with surface markers, fixed and permeabilized by Fixation and Permeabilization buffer (BD Bioscience, #554722). Then, they were stained with anti-p47phox (NCF1, D-10), anti-p67phox (NCF2, D-6) and anti-p40phox (NCF4, D-8) (all from Santa Cruz). Samples without staining the targeted protein, which were indicated as fluorescence minus one (FMO), were used as the negative controls. After that, cells were washed, acquired with Attune NxT flow cytometer (ThermoFisher) and analyzed by Flowjo.10.6.

### 5.3. ROS detection

Intracellular ROS was detected by flow cytometry. Briefly, cells were first stained with cell surface markers, then incubated with 3  $\mu$ M dihydrorhodamine (DHR) 123 (Invitrogen, #D23806) for 10 min at 37 °C and stimulated with 200 ng/ml PMA (Sigma-Aldrich, #P1585) for 20 min at 37 °C. Dimethyl sulfoxide (DMSO) (Molecular Probes, #L34976B) was used for control group. Geometric mean fluorescence intensity (MFI) of DHR was detected by flow cytometry.

Extracellular ROS production was detected by chemiluminescence assay. Briefly, cells were stimulated with 100 ng/ml PMA for 60 min in HBSS (with  $\text{Ca}^{2+}$  and  $\text{Mg}^{2+}$ ) (ThermoFisher, #14025050) containing 150  $\mu$ M isoluminol (Sigma-Aldrich, #A8264) and 18.75U/ml HRP II (Sigma-Aldrich, #P8250). Cells without PMA stimulation were used as negative controls. Data output was measured in relative light units (RLU).

### 5.4. Induction and evaluation of collagen-induced arthritis (CIA)

Rat type II collagen (COL2) was obtained from pepsin-digested SWARM chondrosarcoma, and subsequently processed as previously described [46]. Mice were immunized with rat COL2 (1 mg/ml, 100 mg per mouse) emulsified 1:1 in 50  $\mu$ l complete Freund's adjuvant (CFA, Nordic Biolabs #263810) intradermally at the base of tail. When indicated in the figure, they were boosted on the 35th day after primary immunization with rat COL2 emulsified 1:1 in incomplete Freund's adjuvant (IFA, Nordic Biolabs #263910) in a total volume of 50  $\mu$ l. All experiments were performed blindly, with age and sex-matched

littermates and with groups randomly distributed in cages.

Arthritis severity was scored using a macroscopic scoring system [47] blindly at the indicated time points after primary immunization. Briefly, 1 point was given for one red and swelling finger/toe, 1–5 points were given for each inflamed ankle/wrist or paw/hand according to the severity. A total of 15 points could be given to one limb and all mice were scored arrange from 0 to 60 points. Mice were bled from the sub-mandibular vein at indicated time points in order to detect anti-COL2 antibodies by ELISA. Briefly, serum was diluted and added to COL2-coated (10  $\mu$ g/ml) ELISA plates (Biolegend, #423501). Bound Igs were detected with HRP-conjugated goat anti-mouse Ig kappa (Southern Biotech, #1170-05) or anti indicated isotypes of mouse Igs (anti-IgG1 [#1070-05], anti-IgG2b [#1091-05], anti-IgG2c [#1078-05], anti-IgM [#1021-05], all from Southern Biotech) and ABTS (Roche, #11112422001). The absorbance was read at 405nm (Synergy-2; Bio-Tek Instruments). For total anti-COL2 antibodies, recombinant anti-COL2 antibody (0.1 mg/ml, homemade) was used as standard. All animal experiments were performed under valid ethical permits approved by animal welfare authorities (Stockholm region, Sweden).

### 5.5. Antigen-specific antibody secreting cells detection

Single cell suspension was obtained from spleen, lymph nodes, bone marrow, synovium and resuspended in complete RPMI (ThermoFisher, #61870044) media containing 10% FCS (ThermoFisher, #26140079) and penicillin/streptomycin (Sigma, #P4333). Then, cells were added into COL2-coated (10  $\mu$ g/ml), dsDNA-coated (20  $\mu$ g/ml, Sigma-Aldrich, #D3664), nucleosome-coated (10  $\mu$ g/ml, homemade) or anti-IgG-coated (1  $\mu$ g/ml) ELISPOT plates (Merck Millipore, #MSIPS4W10). For dsDNA coating, Poly-L-Lysine (20  $\mu$ g/ml, #P2658) was pre-coated one day before and dsDNA was coated in sterile TE buffer. After 2 h incubation at 37 °C, plates were washed and detected by biotinylated goat anti-mouse IgG (Southern Biotech, #1030-08), IgG1 (Southern Biotech, #1070-08) or IgG2b (Southern Biotech, #1090-08), followed by ExtrAvidin® conjugated alkaline phosphatase (Sigma-Aldrich, #E2636) and BCIP/NBT (Sigma-Aldrich, #B5655). Spots were scanned with ImmunoScan and analyzed with ImmunoSpot software (Cellular Technology Ltd.).

### 5.6. T cell recall assay

Peptides spanning the sequence 259–273 of COL2 with a non-modified lysine at position 264 (K264) or with a  $\beta$ -D-galactopyranosyl residue on L-hydroxylysine at position 264 (GalHyK264) were synthesized as previously described [48]. Cells from spleen and inguinal lymph nodes were subjected to anti-IFN $\gamma$  (AN18) (Mabtech, #3321-3-1000), anti-IL17A (TC11-18H10.1) (BD, #555068), anti-IL4 (11B11) (BD, #554434) (5  $\mu$ g/ml) pre-coated ELISPOT plates and stimulated with the GalHyK264 peptide for 24 h. Bound cytokines were detected with biotinylated anti-IFN $\gamma$  (R46-A2) (Mabtech, #3321-6-1000) or anti-IL17A (TC11-8H4) (Biolegend, #507002) or anti-IL4 (BVD6-24G2) (BD, #554390) (1  $\mu$ g/ml) and ExtrAvidin conjugated alkaline phosphatase. Spots were developed with BCIP/NBT. Scanned wells were analyzed with ImmunoSpot software.

### 5.7. Antigen presentation assays

Splenocytes were co-cultured with COL2-specific T cell hybridoma (HCQ.3 or HCQ.4 hybridoma) cells for 24 h in the presence of heat-denatured COL2 (using HCQ.3), K264 (using HCQ.4) or GalHyK264 peptide (using HCQ.3). IL2 production in the supernatant was detected by ELISA. Briefly, culture supernatant was subjected to anti-IL2 (Jes6-1A12, homemade, 1  $\mu$ g/ml) pre-coated plates, and captured IL2 was detected by biotinylated anti-IL2 (Jes6-5H4, homemade, 1  $\mu$ g/ml) with Eu-labeled streptavidin (PerkinElmer, #1244-360) and measured by dissociation-enhanced time-resolved fluorometry (excitation 360/40 and emission 620/40, Synergy-2; BioTek Instruments). Recombinant

murine IL2 (Peprotech, #212-12) was used as standard.

### 5.8. B cell isolation and *in vitro* differentiation

B cells were isolated by magnetic-activated cell sorting (MACS) techniques following the protocol provided by Miltenyi Biotec (Order no.130-121-30, CD19 MicroBeads, mouse). Briefly, splenocytes were resuspended in MACS buffer and incubated with CD19 MicroBeads for 10 min, then subjected to pre-rinsed LS column (Miltenyi Biotec, #130-042-401). After washing with MACS buffer for 3 times, B cells were eluted by flushing 5 ml of MACS buffer using the plunger, then resuspended in complete RPMI supplemented with 10% FCS and penicillin/streptomycin.

For lipopolysaccharide (LPS) stimulation, B cells were cultured in TC-treated 96 well U-bottom plates (Falcon®, #353077) in complete RPMI media further supplemented with 10 µg/ml LPS (Sigma-Aldrich, #L2880) for 84 h. 10 µM hydrogen peroxide (H<sub>2</sub>O<sub>2</sub>, Sigma-Aldrich, #H3410) and 10 µM GSK (GSK2795039, Sigma-Aldrich, #SML2770) were added in after 40 h incubation. For CD40L stimulation, B cells were cultured 84 h in CD40L expressing irradiated (50 Gy) fibroblasts (kind gift from Rita Carsetti, B Cell Pathophysiology Unit, Immunology Research Area, Bambino Gesù Children's Hospital IRCCS, 00146 Rome, Italy) pre-coated TC-treated 96 well U-bottom plates, and further supplemented with 50 ng/ml murine IL21 (Peprotech, #210-21), with or without 50 ng/ml murine IL4 (Peprotech, #214-14) with or without 5 µg/ml goat anti-mouse IgM (Fab)<sup>2</sup> (anti-µ) (Jackson Immuno Research, #115-006-075) as indicated. Cells were cultured at 37 °C in humidified air with 5% CO<sub>2</sub>. Culture supernatants were aspirated carefully and checked for total IgM antibodies. Cells were collected for flow cytometric analysis.

### 5.9. B cell transfer experiment

B cells were MACS-sorted from spleens of male B6NQ.Cd45<sup>1</sup> mice, male B10Q.Cd45<sup>2</sup>.Ncf4<sup>58A/58A</sup> and male B10Q.Cd45<sup>2</sup>.Ncf4<sup>R58/R58</sup> mice then adjusted to the same concentration in PBS (Thermo fisher, #14190169). For chimeric B cell transfer experiment (performed in Fig. 5A–G), CD45.1<sup>+</sup> B cells (from B6NQ.Cd45<sup>1</sup> mice) and CD45.2<sup>+</sup> B cells (from B10Q.Ncf4<sup>58A/58A</sup> or B10Q.Ncf4<sup>R58/R58</sup> mice) were equally mixed and transferred to recipient B10Q.µMt.Ncf4<sup>58A/58A</sup> mice intravenously. For experiments performed in Fig. 5H, B cells were mixed and transferred to recipient B10Q.µMt.Ncf4<sup>58A/58A</sup> mice separately. A total of 10 million B cells were transferred to each recipient mouse. B cell viability and purity after sorting were checked by flow cytometry. Blood from recipient mice was taken for checking the transfer efficacy. 2 days after transfer, mice were induced CIA following the protocol described above (without boost).

### 5.10. Statistical analysis

Experiments pooled had balanced groups and no data has been excluded. Data were expressed as mean ± SEM and analyzed using GraphPad Prism (Version 8.0). Mann-Whitney test was employed to analyze significant differences between two groups. Kruskal-Wallis test and Dunn's multiple comparisons test were used for comparing differences between three groups. Pearson correlation analysis was used to analyze correlation between antibody titers and disease severity. Multiple Student's t tests with Holm-Sidak's comparison correction were used to determine the significant differences in the disease severity and incidence of CIA on different DPIs. P-values smaller than the significance level (set to 0.05) are indicated by asterisks (\**p*<0.05, \*\**p*<0.01, \*\*\**p*<0.001, and \*\*\*\**p*<0.0001).

### Author contributions

CH designed the research, performed most of the experiments,

including acquiring and analyzing data. HL contributed with PIL related experiments and part of *in vitro* experiments. AC, ML and QL contributed with part of long-term CIA experiments. AK provided the irradiated CD40L expressing fibroblasts and contributed with designing the *in vitro* experiment. JX, SM and ZY contributed with experiments design and manuscript revision. R.H. designed the research, analyzed the data, revised the manuscript, supervised, and takes the overall responsibility of the study. All authors revised and approved the manuscript.

### Declaration of competing interest

The authors declare no competing financial interests.

### Acknowledgments

We thank Phillip T. Hawkins for kindly sharing the Ncf4<sup>R58A/R58A</sup> mice. We thank Rita Carsetti for generously providing the CD40L expressing fibroblasts. We thank Bingze Xu for producing rat and bovine COL2 as well as all homemade antibodies. We thank Jenny Björklund and Carlos Palestro for the animal management and handling. This work was supported by grants from Knut and Alice Wallenberg foundation (2019.0059), Vetenskapsrådet (2019-01209) and National Natural Science Foundation of China (No. 32070913).

### Appendix A. Supplementary data

Supplementary data to this article can be found online at <https://doi.org/10.1016/j.redox.2022.102422>.

### References

- [1] M.C. Dinauer, S.H. Orkin, R. Brown, A.J. Jesaitis, C.A. Parkos, The glycoprotein encoded by the X-linked chronic granulomatous disease locus is a component of the neutrophil cytochrome b complex, *Nature* 327 (6124) (1987) 717–720.
- [2] O. Sareila, T. Kelkka, A. Pizzolla, M. Hultqvist, R. Holmdahl, NOX2 complex-derived ROS as immune regulators, *Antioxidants Redox Signal.* 15 (8) (2011) 2197–2208.
- [3] T. Ueyama, T. Tatsuno, T. Kawasaki, S. Tsujibe, Y. Shirai, H. Sumimoto, T.L. Leto, N. Saito, A regulated adaptor function of p40phox: distinct p67phox membrane targeting by p40phox and by p47phox, *Mol. Biol. Cell* 18 (2) (2007) 441–454.
- [4] R.V. Stahelin, A. Burian, K.S. Bruzik, D. Murray, W. Cho, Membrane binding mechanisms of the PX domains of NADPH oxidase p40phox and p47phox, *J. Biol. Chem.* 278 (16) (2003) 14469–14479.
- [5] P. Stampoulis, T. Ueda, M. Matsumoto, H. Terasawa, K. Miyano, H. Sumimoto, I. Shimada, Atypical membrane-embedded phosphatidylinositol 3,4-bisphosphate (PI(3,4)P<sub>2</sub>)-binding site on p47(phox) Phox homology (PX) domain revealed by NMR, *J. Biol. Chem.* 287 (21) (2012) 17848–17859.
- [6] Z.M. Song, L. Bouchab, E. Hudik, R. Le Bars, O. Nusse, S. Dupre-Crochet, Phosphoinositol 3-phosphate acts as a timer for reactive oxygen species production in the phagosome, *J. Leukoc. Biol.* 101 (5) (2017) 1155–1168.
- [7] J.D. Pollock, D.A. Williams, M.A. Gifford, L.L. Li, X. Du, J. Fisherman, S.H. Orkin, C.M. Doerschuk, M.C. Dinauer, Mouse model of X-linked chronic granulomatous disease, an inherited defect in phagocyte superoxide production, *Nat. Genet.* 9 (2) (1995) 202–209.
- [8] A. van de Geer, A. Nieto-Patlan, D.B. Kuhns, A.T. Tool, A.A. Arias, M. Bouaziz, M. de Boer, J.L. Franco, R.P. Gazendam, J.L. van Hamme, M. van Houdt, K. van Leeuwen, P.J. Verkuijlen, T.K. van den Berg, J.F. Alzate, C.A. Arango-Franco, V. Batura, A.R. Bernasconi, B. Boardman, C. Booth, S.O. Burns, F. Cabarcas, N. C. Bensusan, F. Charbit-Henrion, A. Corveleyn, C. Deswarte, M.E. Azcoiti, D. Foell, J.J. Gallin, C. Garces, M. Guedes, C.H. Hinze, S.M. Holland, S.M. Hughes, P. Ibanez, H.L. Malech, I. Meyts, M. Moncada-Velez, K. Moriya, E. Neves, M. Oleastro, L. Perez, V. Rattina, C. Oleaga-Quintas, N. Warner, A.M. Muise, J.S. Lopez, E. Trindade, J. Vasconcelos, S. Vermeire, H. Wittkowski, A. Worth, L. Abel, M. C. Dinauer, P.D. Arkwright, D. Roos, J.L. Casanova, T.W. Kuijpers, J. Bustamante, Inherited p40phox deficiency differs from classic chronic granulomatous disease, *J. Clin. Invest.* 128 (9) (2018) 3957–3975.
- [9] J.D. Matute, A.A. Arias, N.A. Wright, I. Wrobel, C.C. Waterhouse, X.J. Li, C. C. Marchal, N.D. Stull, D.B. Lewis, M. Steele, J.D. Kellner, W. Yu, S.O. Meroueh, W. M. Nauseef, M.C. Dinauer, A new genetic subgroup of chronic granulomatous disease with autosomal recessive mutations in p40 phox and selective defects in neutrophil NADPH oxidase activity, *Blood* 114 (15) (2009) 3309–3315.
- [10] L.M. Olsson, C. Johansson Å, B. Gullstrand, A. Jönsen, S. Saevarsdottir, L. Rönnblom, D. Leonard, J. Wetterö, C. Sjöwall, E. Svenungsson, I. Gunnarsson, A. A. Bengtsson, R. Holmdahl, A single nucleotide polymorphism in the NCF1 gene leading to reduced oxidative burst is associated with systemic lupus erythematosus, *Ann. Rheum. Dis.* 76 (9) (2017) 1607–1613.

- [11] L.M. Olsson, A. Nerstedt, A.K. Lindqvist, S.C. Johansson, P. Medstrand, P. Olofsson, R. Holmdahl, Copy number variation of the gene NCF1 is associated with rheumatoid arthritis, *Antioxidants Redox Signal.* 16 (1) (2012) 71–78.
- [12] J. Zhao, J. Ma, Y. Deng, J.A. Kelly, K. Kim, S.Y. Bang, H.S. Lee, Q.Z. Li, E. K. Wakeland, R. Qiu, M. Liu, J. Guo, Z. Li, W. Tan, A. Rasmussen, C.J. Lessard, K. L. Sivils, B.H. Hahn, J.M. Grossman, D.L. Kamen, G.S. Gilkeson, S.C. Bae, P. M. Gaffney, N. Shen, B.P. Tsao, A missense variant in NCF1 is associated with susceptibility to multiple autoimmune diseases, *Nat. Genet.* 49 (3) (2017) 433–437.
- [13] L.M. Olsson, A.K. Lindqvist, H. Kallberg, L. Padyukov, H. Burkhardt, L. Alfredsson, L. Klareskog, R. Holmdahl, A case-control study of rheumatoid arthritis identifies an associated single nucleotide polymorphism in the NCF4 gene, supporting a role for the NADPH-oxidase complex in autoimmunity, *Arthritis Res. Ther.* 9 (5) (2007) R98.
- [14] T.P. Zhang, R. Li, Q. Huang, H.F. Pan, D.Q. Ye, X.M. Li, Association of NCF2, NCF4, and CYBA gene polymorphisms with rheumatoid arthritis in a Chinese population, *J Immunol Res* (2020), 8528976, 2020.
- [15] P. Olofsson, J. Holmberg, J. Tordsson, S. Lu, B. Åkerström, R. Holmdahl, Positional identification of Ncf1 as a gene that regulates arthritis severity in rats, *Nat. Genet.* 33 (1) (2003) 25–32.
- [16] M. Hultqvist, O. Sareila, F. Vilhardt, U. Norin, L.M. Olsson, P. Olofsson, U. Hellman, R. Holmdahl, Positioning of a polymorphic quantitative trait nucleotide in the Ncf1 gene controlling oxidative burst response and arthritis severity in rats, *Antioxidants Redox Signal.* 14 (12) (2011) 2373–2383.
- [17] T. Kelkka, D. Kienhofer, M. Hoffmann, M. Linja, K. Wing, O. Sareila, M. Hultqvist, E. Laajala, Z. Chen, J. Vasconcelos, E. Neves, M. Guedes, L. Marques, G. Kronke, M. Helminen, L. Kainulainen, P. Olofsson, S. Jalkanen, R. Lahesmaa, M.M. Souto-Carneiro, R. Holmdahl, Reactive oxygen species deficiency induces autoimmunity with type 1 interferon signature, *Antioxidants Redox Signal.* 21 (16) (2014) 2231–2245.
- [18] C.O. Jacob, M. Eisenstein, M.C. Dinuer, W. Ming, Q. Liu, S. John, F. P. Quismorio Jr., A. Reiff, B.L. Myones, K.M. Kaufman, D. McCurdy, J.B. Harley, E. Silverman, R.P. Kimberly, T.J. Vyse, P.M. Gaffney, K.L. Moser, M. Klein-Gitelman, L. Wagner-Weiner, C.D. Langefeld, D.L. Armstrong, R. Zidovetzki, Lupus-associated causal mutation in neutrophil cytosolic factor 2 (NCF2) brings unique insights to the structure and function of NADPH oxidase, *Proc. Natl. Acad. Sci. U. S. A.* 109 (2) (2012) E59–E67.
- [19] W. Tian, X.J. Li, N.D. Stull, W. Ming, C.I. Suh, S.A. Bissonnette, M.B. Yaffe, S. Grinstein, S.J. Atkinson, M.C. Dinuer, Fc gamma R-stimulated activation of the NADPH oxidase: phosphoinositide-binding protein p40phox regulates NADPH oxidase activity after enzyme assembly on the phagosome, *Blood* 112 (9) (2008) 3867–3877.
- [20] J. Bagaitkar, E.A. Barbu, L.J. Perez-Zapata, A. Austin, G. Huang, S. Pallat, M. C. Dinuer, PI(3)P-p40phox binding regulates NADPH oxidase activation in mouse macrophages and magnitude of inflammatory responses in vivo, *J. Leukoc. Biol.* 101 (2) (2017) 449–457.
- [21] S. Winter, M. Hultqvist Hopkins, F. Laulund, R. Holmdahl, A reduction in intracellular reactive oxygen species due to a mutation in NCF4 promotes autoimmune arthritis in mice, *Antioxidants Redox Signal.* 25 (18) (2016) 983–996.
- [22] D.C. Nguyen, C.J. Joyner, I. Sanz, F.E. Lee, Factors affecting early antibody secreting cell maturation into long-lived plasma cells, *Front. Immunol.* 10 (2019) 2138.
- [23] S. Jafri, S.D. Moore, N.W. Morrell, M.L. Ormiston, A sex-specific reconstitution bias in the competitive CD45.1/CD45.2 congenic bone marrow transplant model, *Sci. Rep.* 7 (1) (2017) 3495.
- [24] S. Basu, A. Ray, B.N. Dittel, Differential representation of B cell subsets in mixed bone marrow chimera mice due to expression of allelic variants of CD45 (CD45.1/CD45.2), *J. Immunol. Methods* 396 (1–2) (2013) 163–167.
- [25] Y.J. Ha, J.R. Lee, Role of TNF receptor-associated factor 3 in the CD40 signaling by production of reactive oxygen species through association with p40phox, a cytosolic subunit of nicotinamide adenine dinucleotide phosphate oxidase, *J. Immunol.* 172 (1) (2004) 231–239.
- [26] M. Bertolotti, S.H. Yim, J.M. Garcia-Manteiga, S. Masciarelli, Y.J. Kim, M.H. Kang, Y. Iuchi, J. Fujii, R. Vené, A. Rubartelli, S.G. Rhee, R. Sitia, B- to plasma-cell terminal differentiation entails oxidative stress and profound reshaping of the antioxidant responses, *Antioxidants Redox Signal.* 13 (8) (2010) 1133–1144.
- [27] E.J. Kunkel, E.C. Butcher, Plasma-cell homing, *Nat. Rev. Immunol.* 3 (10) (2003) 822–829.
- [28] C. Ellson, K. Davidson, K. Anderson, L.R. Stephens, P.T. Hawkins, PtdIns3P binding to the PX domain of p40phox is a physiological signal in NADPH oxidase activation, *EMBO J.* 25 (19) (2006) 4468–4478.
- [29] M. Hultqvist, J. Bäcklund, K. Bauer, K.A. Gelderman, R. Holmdahl, Lack of reactive oxygen species breaks T cell tolerance to collagen type II and allows development of arthritis in mice, *J. Immunol.* 179 (3) (2007) 1431–1437.
- [30] K.A. Gelderman, M. Hultqvist, J. Holmberg, P. Olofsson, R. Holmdahl, T cell surface redox levels determine T cell reactivity and arthritis susceptibility, *Proc. Natl. Acad. Sci. U. S. A.* 103 (34) (2006) 12831–12836.
- [31] V.L. Crotzer, J.D. Matute, A.A. Arias, H. Zhao, L.A. Quilliam, M.C. Dinuer, J. S. Blum, Cutting edge: NADPH oxidase modulates MHC class II antigen presentation by B cells, *J. Immunol.* 189 (8) (2012) 3800–3804.
- [32] R.A. Elsner, M.J. Shlomchik, Germinal center and extrafollicular B cell responses in vaccination, immunity, and autoimmunity, *Immunity* 53 (6) (2020) 1136–1150.
- [33] F. Ho, J.E. Lortan, I.C. MacLennan, M. Khan, Distinct short-lived and long-lived antibody-producing cell populations, *Eur. J. Immunol.* 16 (10) (1986) 1297–1301.
- [34] C.P. Marques, P. Kapil, D.R. Hinton, C. Hindinger, S.L. Nutt, R.M. Ransohoff, T. W. Phares, S.A. Stohlman, C.C. Bergmann, CXCR3-dependent plasma blast migration to the central nervous system during viral encephalomyelitis, *J. Virol.* 85 (13) (2011) 6136–6147.
- [35] Y. Akiyama, T. Morikawa, D. Maeda, Y. Shintani, A. Niimi, A. Nomiya, A. Nakayama, Y. Igawa, M. Fukayama, Y. Homma, Increased CXCR3 expression of infiltrating plasma cells in hunner type interstitial cystitis, *Sci. Rep.* 6 (2016), 28652.
- [36] M. Henneken, T. Dörner, G.R. Burmester, C. Berek, Differential expression of chemokine receptors on peripheral blood B cells from patients with rheumatoid arthritis and systemic lupus erythematosus, *Arthritis Res. Ther.* 7 (5) (2005) R1001–R1013.
- [37] D. Cao, I. Khmaladze, H. Jia, E. Bajtner, K.S. Nandakumar, T. Blom, J.A. Mo, R. Holmdahl, Pathogenic autoreactive B cells are not negatively selected toward matrix protein collagen II, *J. Immunol.* 187 (9) (2011) 4451–4458.
- [38] M. Bertolotti, G. Farinelli, M. Galli, A. Aiuti, R. Sitia, AQP8 transports NOX2-generated H<sub>2</sub>O<sub>2</sub> across the plasma membrane to promote signaling in B cells, *J. Leukoc. Biol.* 100 (5) (2016) 1071–1079.
- [39] P. Castellani, G. Angelini, L. Delfino, A. Matucci, A. Rubartelli, The thiol redox state of lymphoid organs is modified by immunization: role of different immune cell populations, *Eur. J. Immunol.* 38 (9) (2008) 2419–2425.
- [40] K. Kwak, M. Akkaya, S.K. Pierce, B cell signaling in context, *Nat. Immunol.* 20 (8) (2019) 963–969.
- [41] H. Zhang, L. Wang, Y. Chu, Reactive oxygen species: the signal regulator of B cell, *Free Radic. Biol. Med.* 142 (2019) 16–22.
- [42] Y.Y. Feng, M. Tang, M. Suzuki, C. Gunasekara, Y. Anbe, Y. Hiraoka, J. Liu, H. Grasberger, M. Ohkita, Y. Matsumura, J.Y. Wang, T. Tsubata, Essential role of NADPH oxidase-dependent production of reactive oxygen species in maintenance of sustained B cell receptor signaling and B cell proliferation, *J. Immunol.* 202 (9) (2019) 2546–2557.
- [43] S.M. Richards, E.A. Clark, BCR-induced superoxide negatively regulates B-cell proliferation and T-cell-independent type 2 Ab responses, *Eur. J. Immunol.* 39 (12) (2009) 3395–3403.
- [44] M.L. Wheeler, A.L. Defranco, Prolonged production of reactive oxygen species in response to B cell receptor stimulation promotes B cell activation and proliferation, *J. Immunol.* 189 (9) (2012) 4405–4416.
- [45] C. Kilkenny, W.J. Browne, I.C. Cuthill, M. Emerson, D.G. Altman, Improving bioscience research reporting: the ARRIVE guidelines for reporting animal research, *PLoS Biol.* 8 (6) (2011), e1000412.
- [46] M. Andersson, R. Holmdahl, Analysis of type II collagen-reactive T cells in the mouse. I. Different regulation of autoreactive vs. non-autoreactive anti-type II collagen T cells in the DBA/1 mouse, *Eur. J. Immunol.* 20 (5) (1990) 1061–1066.
- [47] M. Hultqvist, P. Olofsson, J. Holmberg, B.T. Bäckström, J. Tordsson, R. Holmdahl, Enhanced autoimmunity, arthritis, and encephalomyelitis in mice with a reduced oxidative burst due to a mutation in the Ncf1 gene, *Proc. Natl. Acad. Sci. U. S. A.* 101 (34) (2004) 12646–12651.
- [48] E. Michaëlsson, M. Andersson, A. Engström, R. Holmdahl, Identification of an immunodominant type-II collagen peptide recognized by T cells in H-2q mice: self tolerance at the level of determinant selection, *Eur. J. Immunol.* 22 (7) (1992) 1819–1825.